Properties of the 4.77- and 5.16-MeV States of B^{10}†

D. E. ALBURGER, P. D. PARKER, AND D. J. BREDIN*
Brookhaven National Laboratory, Upton, New York

AND

D. H. WILKINSON
Brookhaven National Laboratory, Upton, New York and Nuclear Physics Laboratory, Oxford, England

AND

P. F. DONOVAN
Bell Telephone Laboratories, Murray Hill, New Jersey and Brookhaven National Laboratory, Upton, New York

AND

A. GALLMANN AND R. E. PIXLEY‡
Institut de Recherches Nucléaires, Strasbourg, France

AND

L. F. CHASE, JR., AND R. E. MCDONALD
Lockheed Missiles and Space Company, Palo Alto, California

(Received 18 October 1965)

The energy levels in B^{10} at 4.77 and 5.16 MeV have been studied by means of the reactions $B^{11}(He^3,\alpha)B^{10}$ and $Li^6(\alpha,\gamma)B^{10}$. In measurements on the $B^{11}(He^3,\alpha)B^{10}$ reaction ($E_{He^3}=3.5$ MeV), alpha particles populating states of B^{10} were observed at 90° in coincidence with (a) B^{10} recoil nuclei, (b) B^{10} recoils and gamma rays, and (c) decay alpha particles, by using two solid-state detectors and a NaI detector. Relative alpha-particle and gamma-ray branching intensities were determined for the decay of the 4.77- and 5.16-MeV states. The ratio of population intensities of the 5.16- and 5.11-MeV states was measured by using a Buechner-type magnetic spectrograph. In the $Li^6(\alpha,\gamma)B^{10}$ reaction thick-target gamma-ray yields were measured at resonances for forming the 4.77- and 5.16-MeV states. For the 4.77-MeV state the angular distribution of the predominant 4.05-MeV gamma ray was determined, the 4.77-MeV ground-state transition was detected, and the angular distribution of the 4.77-MeV gamma ray was measured. The intensity of the ground-state gamma-ray branch from the 4.77-MeV level was measured to be $(0.5\pm0.1)\%$, and the angular distribution of this transition in the $Li^6(\alpha,\gamma)B^{10}$ reaction favors an assignment of $J^\pi=3^+$ to the 4.77-MeV state. Assignments of either $J^\pi=2^+$ or 3^+ are allowed by the angular distribution of the 4.05-MeV transition from this state. Γ_γ/Γ for the 4.77-MeV level was measured to be $(2.3\pm0.3)\times10^{-3}$. For the $J^\pi=3^+$ assignment, partial widths for the 4.77-MeV level were measured to be $\Gamma_\gamma=0.033\pm0.006$ eV and $\Gamma_\alpha=14\pm3$ eV. The partial widths of the 5.16-MeV level were measured as $\Gamma_\gamma=2.9\pm1.1$ eV and $\Gamma_\alpha=0.44\pm0.09$ eV for an alpha-particle branch of $(13\pm4)\%$. The properties of these and neighboring states are discussed in terms of the independent-particle model. Good agreement is found on some striking features but several points remain to be clarified.

I. INTRODUCTION

THE independent-particle model (IPM) has enjoyed enormous success in the $1p$ shell. With the well-known exception of the $E2$ transitions, which clearly demand some form of collective effect, perhaps to be introduced into the model explicitly via configuration mixing or via some cruder technique such as weak surface coupling, rather uniform success has been obtained in the description of low-lying states. The success has extended to dynamical properties, particularly beta decay and $M1$ transitions. It is, of course, essential that a model should describe the dynamics as well as the statics if it is to be acceptable. It is not good enough if it accounts for the level schemes but generates wave functions that fail badly to give an account of transition rates, particularly of strong transitions where chance near-cancellation cannot be invoked.

We now have two types of IPM available. The older type, IPM_{old}, is represented by the work particularly of Inglis[1] and Kurath.[2,3] It uses explicit single-particle wave functions and a purely central residual nucleon-nucleon interaction of chosen exchange mixture. In addition to the over-all shell-model potential that generates the single-particle wave functions and the residual interaction there is a spin-orbit term of the form $a\mathbf{l}\cdot\mathbf{s}$ acting on each nucleon. The traditional procedure has been to commit oneself to the exchange mixture, to the single-particle radial wave functions, usually of harmonic-oscillator type, and to a form and range of the residual interaction. This fixes the ratio L/K of the direct to exchange integrals of the residual interaction. The magnitude of K, treated as a free

† Research at Brookhaven National Laboratory carried out under the auspices of the U. S. Atomic Energy Commission.
* Now at Rutgers University, New Brunswick, New Jersey.
‡ Now at University of Zürich, Zürich, Switzerland.

[1] D. R. Inglis, Rev. Mod. Phys. **25**, 390 (1953).
[2] D. Kurath, Phys. Rev. **101**, 216 (1956).
[3] D. Kurath, Phys. Rev. **106**, 975 (1957).

parameter, is then a measure of the strength of the residual interaction and sets the energy scale for the calculated level schemes. The level schemes, apart from their energy scale, depend only on a/K, the intermediate-coupling parameter. a couples **s** to **l** and K measures the orbit-orbit interaction so $a/K=0$ is the LS limit and $a/K=\infty$ is the jj limit. In this approach the free parameters are a/K and K which are allowed to vary from nucleus to nucleus to get the best fit to each level scheme. It is satisfactory that these best fits are found for values of K that are essentially constant through the shell corresponding to the fact that the nuclear size is rather constant through the shell while a/K changes rather smoothly with A from close to the LS limit at the beginning of the shell to close to the jj limit at the end. Of course, $\mathrm{IPM_{old}}$ contains many more than the two parameters K and a/K but they are frozen into the starting point as described. Although it is perhaps illogical to single out two parameters in this way it has the advantage that one may easily check the effect of varying them and only go back to the starting point if persistent inconsistencies are found. K and a/K are chosen as the free parameters because one believes that it is of them that one has the least *a priori* knowledge. The new approach, $\mathrm{IPM_{new}}$, is radically different. In its extreme form, one uses as free parameters the full 15 matrix elements of the two-nucleon interaction in the $1p$-shell without reference to an explicit residual interaction, single-particle wave functions, or any other detail. These 15 matrix elements plus the two single-particle energies $1p_{3/2}$ and $1p_{1/2}$, that come from interaction with the $1s$ shell, fix all the properties of $1p$-shell states if the assumption is made that they have no A dependence. A simplification is introduced by taking the $1p_{3/2}$ and $1p_{1/2}$ radial wave functions to be the same and by restricting the (unspecified) residual interaction to be symmetric in the spatial coordinates. This facilitates comparison with the phenomenological potentials used to describe nucleon-nucleon scattering which have the same symmetry property. This latter approach has 13 parameters as against the 17 of the first. With these parameters as variables a selected range of "certain" data about the $1p$ shell are fitted by a procedure that minimizes the deviation of the model fit from experiment, thereby fixing the parameters and with them all other $1p$-shell properties. This approach has been applied by Amit and Katz[4] and by Cohen and Kurath.[5] It has the beauty of great generality but the disadvantages of depending for its parameters, and so for its predictions, on the selection of the initial input data and of being opaque: Since all its parameters stand on an equal footing there is no easy way of seeing whether a particular "rogue" level or a particular "rogue" dynamical property is very sensitive to the details of the calculation as there was in $\mathrm{IPM_{old}}$. In $\mathrm{IPM_{old}}$, one simply examined the dependence on a/K, and if it were strong, one argued that a small change in the frozen parameters might bring it into line. In $\mathrm{IPM_{new}}$, the question of rogues can only be properly answered by the much more complicated business of examining their dependence on all the less-well-determined of the 17 or 13 parameters, or by including them in the input data of a complete new parametrization and seeing whether they can be satisfactorily accommodated or whether they disrupt the scheme, give a significantly poorer over-all fit and generate other rogues. However, this apparent defect of opacity is unavoidable if we are to give a satisfactory answer to the question of rogues rather than simply see from their sensitivity to a/K in $\mathrm{IPM_{old}}$ that they can possibly be accommodated in the scheme. We will illustrate this comment immediately from the work we report here. From now on by $\mathrm{IPM_{new}}$ we shall mean the version of Cohen and Kurath.[5]

The case of $A=10$ is an interesting one. This is a "complicated" nucleus, $(1p)^6$, equidistant from the two ends of the $1p$-shell. It was therefore gratifying that $\mathrm{IPM_{old}}$[2] appeared to give an excellent account of the positions of the low-lying levels of even parity that may belong to $(1p)^6$ at least up to and including the seventh, the $J^\pi=2^+$, $T=1$ state at 5.16 MeV. A difficulty was the state at 4.77 MeV. This appeared,[6,7] from the reaction $\mathrm{Li^6}(\alpha,\gamma)\mathrm{B^{10}}$, to be of even parity and of $J=2$ or 3 and so is a candidate for inclusion in $(1p)^6$. However, in the successful parametrization of B^{10} which gave a good account of the other states up to that at 5.16 MeV for $a/K\approx 4.5$, no state of $J=2$ or 3 was available and unaccounted for below the $J^\pi=2^+$, $T=1$ state. States of $J=2$ and 3 were available 1 MeV and more above 4.77 MeV. These states were very sensitive to a/K but could not be brought below the $T=1$ state except at low values of a/K that gave unacceptably poor fits to the lower levels, themselves well fitted at $a/K\approx 4.5$. Another striking feature of the 4.77-MeV state is its decay scheme, in particular the ground-state transition which, it was early apparent,[8] is extremely weak. $\mathrm{IPM_{old}}$, for both spin possibilities $J=2$, 3, predicted a weak $M1$ transition to the ground state as expected from its $T=0\rightarrow T=0$ character, but without the unusual weakness of the experimental transition. The strong energy sensitivity of these states to a/K may suggest that they could be satisfactorily accommodated in the scheme by slight changes of other parameters but we have no assurance of this nor, of course, that the very weak ground-state transition would then be more satisfactorily accounted for.

The situation under $\mathrm{IPM_{new}}$[5] is most interesting. Here the $J=3$ possibility has come down, in the best 17-parameter version using only $A=8$ through 16,

[4] D. Amit and A. Katz, Nucl. Phys. **58**, 388 (1964).
[5] S. Cohen and D. Kurath, Nucl. Phys. **73**, 1 (1965).
[6] L. Meyer-Schützmeister and S. S. Hanna, Phys. Rev. **108**, 1506 (1957).
[7] H. Warhanek, Phil. Mag. **2**, 1085 (1957).
[8] D. H. Wilkinson and G. A. Jones, Phys. Rev. **91**, 1575 (1953).

($IPM_{new(8)}$), to about 4.8 MeV and its ground-state $M1$ transition has become vanishingly small, so fitting the experiment well in both respects. [In ($IPM_{new(6)}$), the 17-parameter version that uses $A=6$ through 16, the state lies at about 5.3 MeV. This is still satisfactory.] The $J=2$ possibility remains somewhat higher in energy and its $M1$ ground-state transition is even stronger than under IPM_{old}. An object of the work reported in this paper is to determine the J^π value of the 4.77-MeV level and to obtain quantitative measures of its dynamical properties to make definite its confrontation with the models.

Of course it could be that the 4.77-MeV level does not belong to $(1p)^6$ and the weakness of its $M1$ transitions to the ground state might be due to this. However, as we shall explain below, the state also exhibits very remarkable collective properties in its $E2$ width to the $J^\pi=1^+$ state at 0.72 MeV and in its alpha-particle decay to the ground state of Li^6. Such properties, particularly $E2$ transitions, when they link a state with states that belong to the IPM as in the case here, usually signal collective enhancement of properties already strongly developed within the IPM framework and are not usually found in states that do not belong in first approximation to that framework.

The other state with which we are concerned here is the important $J^\pi=2^+$, $T=1$ state at 5.16 MeV. It is clear from accurate measurements[9] of the gamma-ray branching ratios that IPM_{old} cannot simultaneously give a good account of the level scheme and of these dynamical properties. It is obviously important in such a case to tie down the disagreement by absolute as well as relative determinations of the radiative widths since agreement with theory for one or two transitions may imply defective or wrongly identified wave functions for states to which the other, discrepant, transitions lead. It is already clear that for this state alpha-particle and gamma-ray emission compete on approximately equal terms; this is not surprising in view of the $T=1$ character of the state. Measurements on the absolute gamma-ray yield in the reaction $Li^6(\alpha,\gamma)B^{10}$ do not, therefore, give Γ_γ and we must independently determine $\Gamma_\gamma/\Gamma_\alpha$. That was a main objective of the work now to be reported. In this case there is no reason why the $M1$ transitions should be weak since $\Delta T=1$ and indeed some are strong according both to IPM_{old} and IPM_{new}. However, both versions of the model also predict certain weak transitions but they are different for the different versions. It is our hope in presenting this work to make a quantitative assessment of the IPM's success and predicament and in particular to determine whether the improvement of IPM_{new} over IPM_{old} noted as likely for the 4.77-MeV level extends to the radiative properties of the 5.16-MeV state.

Figure 1 shows the states of B^{10} and the transitions of chief interest in this work. Included in the figure are some of the results from the present work to be discussed in the following sections.

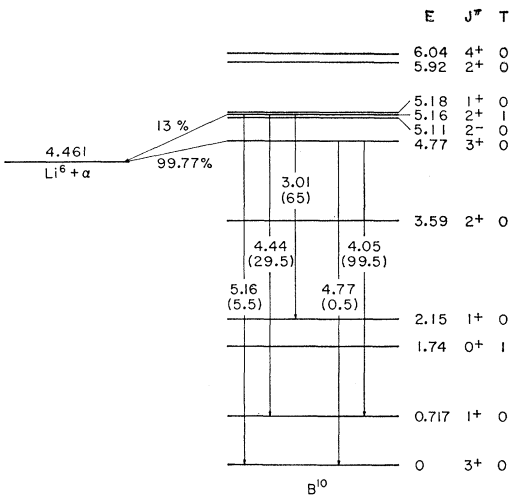

FIG. 1. Energy levels of B^{10}, including some of the results on the 4.77- and 5.16-MeV states from the present work. Numbers in parentheses are the relative percentages of gamma-ray branching.

II. EXPERIMENTAL PROCEDURES AND RESULTS

A. The $B^{11}(He^3,\alpha)B^{10}$ Reaction

Targets for studies of the $B^{11}(He^3,\alpha)B^{10}$ reaction consisted of 50 $\mu g/cm^2$ thick self-supporting foils of enriched (97%)B^{11} which had been prepared by electron-beam evaporation. These were attached to brass washers placed on a rotatable mounting post at the center of a bombardment chamber which has the following features: two arms for mounting detector and slit assemblies, independently rotatable in the horizontal plane from the outside; beam-collimating and current-measuring assemblies; an internal angular scale for reading detector angles; viewing ports for checking beam spot and detector alignment; and a thick Plexiglas lid allowing the angular scale to be viewed and having a 5.5-in.-diameter well at the center. A 5×5-in NaI scintillation crystal can be placed in the well such that the front surface of the crystal is only 2.0 cm from the center of the target.

In all the experiments a 3.5-MeV He^3 beam struck the target after collimation to a diameter of 0.7 or 1.0 mm. Charged-particle spectra were measured using solid-state detectors. Except for the alpha-alpha coincidence measurements described in Sec. II A.2b the detectors were commercial units made by ORTEC with sensitive thicknesses selected to be $\sim 95\ \mu$ so as to prevent protons and deuterons from giving pulses in the spectral region of interest. One detector, designated as the alpha-particle detector, was always positioned at 90° to the beam, and for coincidence runs another detector was located on the opposite side of the beam at appropriate

[9] E. K. Warburton, D. E. Alburger, and D. H. Wilkinson, Phys. Rev. 132, 776 (1963).

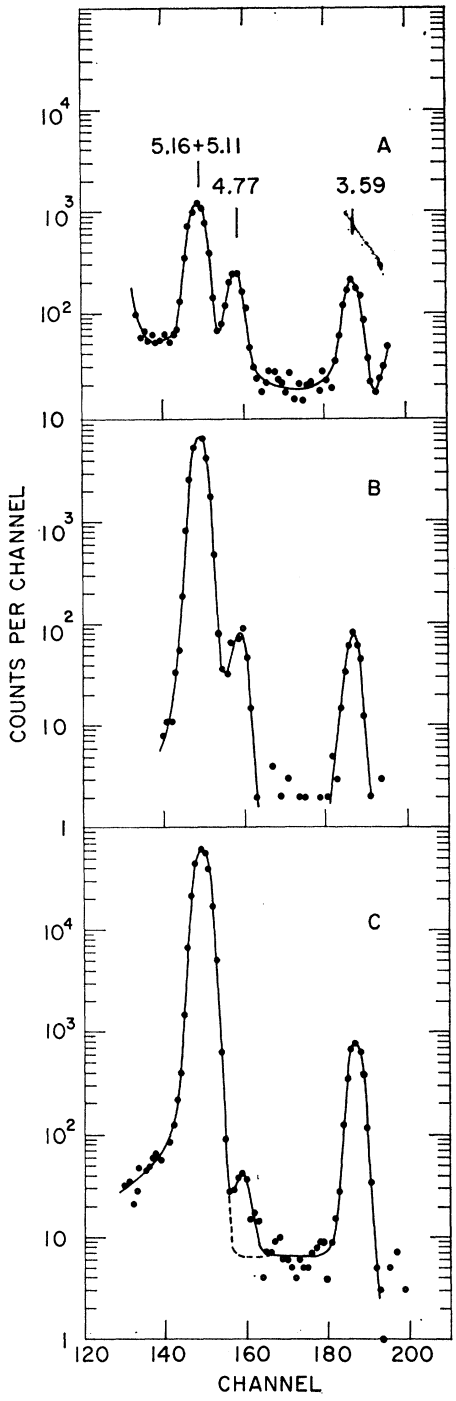

FIG. 2. (A) Curve of alpha-particle singles spectrum from the $B^{11}(He^3,\alpha)B^{10}$ reaction observed at $\theta=90°$ with $E_{He^3}=3.5$ MeV. The slit in front of the silicon detector was 1.5×9 mm² at a distance of 2.5-cm from the target. (B) Curve of alpha particles in coincidence with the recoil detector when the angular position of the recoil detector and the pulse-height window on its output are set for equal efficiency in detecting recoils associated with the 5.16- and 4.77-MeV states. Most of the 4.77-MeV line arises from response of the recoil detector to Li^6 and He^4 breakup products. (C) Curve of alpha particles in triple coincidence with the recoil detector, set as in curve of (B), and with a gamma-ray detector biased to accept pulses of >0.6 MeV.

angles for detecting recoil B^{10} nuclei or decay alpha particles.

Outputs of the two silicon detectors and the NaI detector were amplified and fed to two coincidence units which allowed various combinations of double or triple coincidence events to gate either of two 400-channel pulse-height analyzers or a 1024-channel section of a 16 384-channel pulse-height analyzer.

1. Gamma-Ray Decay of the B^{10} 4.77-MeV Level

For these experiments the slit in front of the alpha-particle detector was 1.5×9 mm² at a distance of 2.5 cm from the center of the target. A portion of the singles spectrum is shown in Fig. 2(A) where the peaks are identified according to the corresponding energy levels in B^{10}.

Attempts were made to observe the gamma-ray decay of the 4.77-MeV level by measuring the alpha particles to this level in coincidence with gamma rays above 0.6 MeV in the 5×5-in. NaI detector. Limitations were imposed both by random coincidences and by the real coincidences due to the low-energy tail of the 3.59-MeV peak. These two effects were about equal in intensity under our experimental conditions. From these data it was only possible to set an upper limit of 1% on the fractional gamma-ray branch.

In order to improve on the sensitivity for finding the gamma-ray decay of the 4.77-MeV level, the additional requirement of a triple coincidence with a second silicon detector was imposed when the latter detector was positioned at the correct kinematic angle to detect the corresponding B^{10} recoil nucleus. Because of the sharp alpha-recoil kinematic correlation it was expected that the real triple-coincidence effect would be an appreciable fraction of the α-γ double-coincidence rate, while the background effects should be considerably smaller.

In considering first the background, due to the tail of the 3.59-MeV peak it may be seen from the kinematic calculations given in Table I that the recoil nuclei

TABLE I. Kinematic calculations of angles and energies of the B^{10} recoil nucleus for various B^{10} energy levels in the reaction $B^{11}(He^3,\alpha)B^{10}$ under the conditions $E_{He^3}=3.50$ MeV and $\theta_\alpha=-90°$.

B^{10} Energy level (MeV)	Angle of B^{10} recoil (deg.)	Energy of B^{10} recoil (MeV)
3.59	55.8	3.33
4.77	53.7	2.99
5.16	52.9	2.88

corresponding to the 4.77- and 3.59-MeV levels are separated by 2° in angle and by 10% in energy. To test what degree of discrimination against the 3.59-MeV tail could be achieved by making use of these differences several types of runs were made on alpha-recoil coincidences associated with the 5.16- and 3.59-MeV levels. Figure 3 shows the alpha-recoil coincidence yield for each of these alpha-particle lines plotted against the

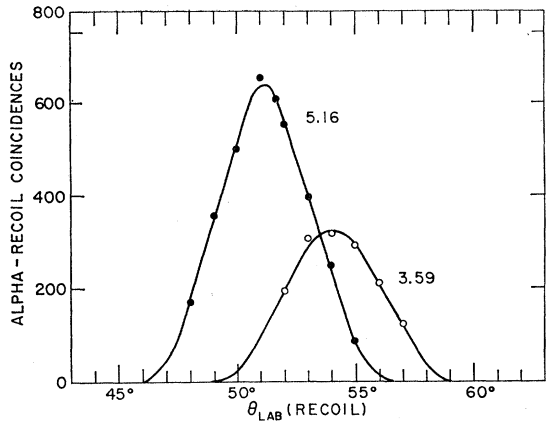

FIG. 3. Coincidences between alpha particles from the $B^{11}(He^3,\alpha)B^{10}$ reaction, observed at $\theta=-90°$, and recoil B^{10} nuclei versus the angle of the recoil detector when channeling on the 5.16- and 3.59-MeV alpha-particle lines. Intensity normalizations are different for the two curves.

angle of the recoil detector. The slit in front of the latter detector was 1.5×9 mm^2 at a distance of 2.25 cm from the target. As expected from the calculations in Table I the peaks in Fig. 3 differ in angle by 3°. Slight differences (about 2°) between the absolute values of the peak angles and the numbers given in Table I are probably accounted for by errors in the alignment of the chamber, the beam spot position, and the locations of the detector slits on the rotatable mounts. The 4.5° full width at half-maximum of the 5.16-MeV curve in Fig. 3 is consistent with the detector-slit geometries, and it indicates that angular spreading associated with target thickness effects is not appreciable. In the final experiments (see below) the recoil detector was set 0.5° away from the center of the 5.16-MeV recoil peak in the direction of the 3.59-MeV peak in Fig. 3. At this position, which is half way between the 5.16-MeV recoil peak and the predicted angle of the 4.77-MeV recoil peak, it is seen from Fig. 3 that the angular discrimination against the 3.59-MeV recoils is approximately a factor of 2.

Further tests were made by setting the recoil detector successively at the 5.16- and 3.59-MeV angular peaks and measuring the pulse-height spectra from this detector in coincidence with windows on the corresponding alpha-particle lines. These results are shown in Figs. 4(A) and 4(B). In Fig. 4(A) the strong main peak is due to B^{10} recoils following the gamma-ray decay of the 5.16-MeV state, while the small peaks at higher energy, discussed in more detail below, are associated with the alpha-particle decays of both the 5.16-MeV state and the unresolved 5.11-MeV level. The recoil peaks in Figs. 4(A) and 4(B) are quite symmetrical, again indicating negligible target thickness effects, and the ratio of the peak channel numbers of 85 and 104 for the 5.16- and 3.59-MeV lines, respectively, agrees well with the energy ratio from Table I. Furthermore, the region of pulse-height overlap of the two recoil curves is such that if a pulse-height window were to be set so as to encompass almost all of the 5.16-MeV recoil peak the window would contain only a few percent of the 3.59-MeV recoils. However, in order to detect the 5.16- and 4.77-MeV recoils with equal efficiency in the coincidence work described below the window on the recoil spectrum was set so that its lower edge was at the low-energy foot of the 5.16-MeV recoil peak in Fig. 4(A) and its upper edge was at the predicted position of the high-energy foot of a 4.77-MeV recoil peak. Under these conditions about $\frac{1}{6}$ of the 3.59-MeV recoil spectrum was included within the window.

By combining the angular and the pulse-height discrimination factors discussed in the foregoing, the over-all factor for discriminating against the 3.59-MeV peak and its low-energy tail was expected to be ~12. The discrimination factor was observed experimentally to be 15 in agreement with the expected factor.

As for the random coincidence contribution, in the alpha-recoil-gamma triple-coincidence measurements, it was expected that if only uncorrelated random coincidences were to occur the random intensity of the 4.77-MeV peak would be extremely small. Such might

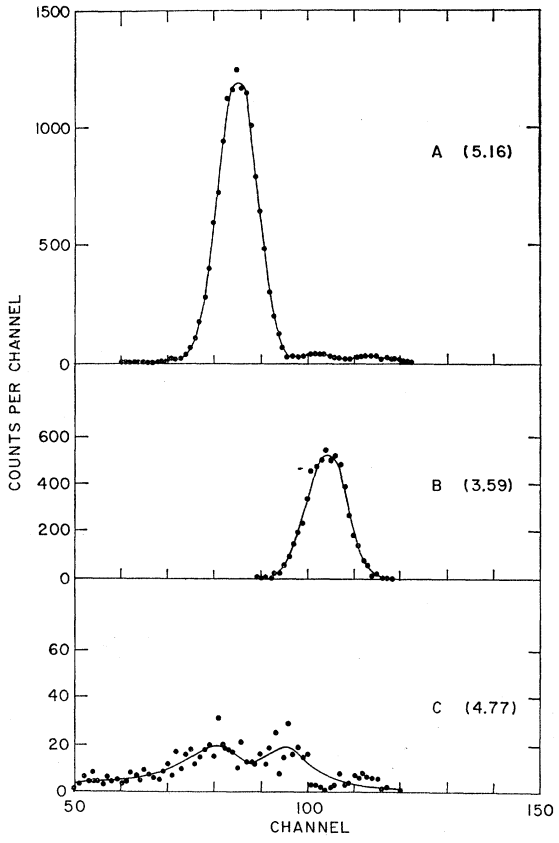

FIG. 4. Recoil-detector pulse-height spectra in coincidence with channels on various alpha-particle lines in the $B^{11}(He^3,\alpha)B^{10}$ reaction. Curves in (A), (B), and (C) are the spectra obtained when the channel was placed on the 5.16-, 3.59-, and 4.77-MeV alpha-particle lines, respectively.

be the case for the 4.77-MeV line if the recoil detector responded only to B^{10} recoil nuclei. However, a comparison of Figs. 4(A), 4(B), and 4(C) shows that for states that decay by alpha-particle emission there are other components in the pulse-height spectrum of the recoil detector which will generate real double-coincidence events. Thus, when the pulse-height window on the recoil detector is set to include the B^{10} recoils associated with the 5.16- and 4.77-MeV states as described above, real double coincidences can still occur between the alpha particles populating the 4.77-MeV state and the breakup products of this state that enter the recoil detector. Furthermore, based on considerations of the various types of effects that make up the random-coincidence counting rate in alpha-recoil-gamma (α-RC-γ) coincidence measurements, it was concluded that the only appreciable source of random counts in the 4.77-MeV triple-coincidence peak (as well as in the 5.16-MeV peak) consists of alpha-recoil real coincidences in random coincidence with the gamma-ray detector. Thus, in the triple-coincidence data the normalization of the random spectrum is found by making a real-to-random ratio measurement on the 5.16-MeV peak when only the gamma-ray pulses are delayed in the coincidence circuit, and the contribution of random coincidences to the alpha-particle spectrum at 90° should have essentially the same spectral shape as the alpha-particle spectrum stored in coincidence with only the recoil detector as illustrated in Fig. 2(B).

Figure 2(C) shows the alpha-particle spectrum from the $B^{11}(He^3,\alpha)B^{10}$ reaction resulting from a 40-h α-RC-γ triple-coincidence run at a beam current of 0.065 μA. The angle of the recoil detector and the pulse-height window on its output were set for equal efficiency in detecting recoils from the 5.16- and 4.77-MeV state while the bias on the NaI detector output was set so as to accept all gamma-ray pulses above 0.60 MeV. The 4.77-MeV line in Fig. 2(C) contains a net area of 159 counts after subtraction of the dashed background curve which was estimated by extrapolations of the 3.59-MeV tail and the high-energy edge of the 5.16-MeV line. Under the 5.16-MeV peak in Fig. 2(C) is a total of 249 000 counts. In a 3-h run on random coincidences, taken with the gamma rays delayed, a real-to-random ratio of 151 was found for the 5.16-MeV peak. By combining this number, the 5.16/4.77 ratio of 69 from Fig. 2(B) and the area under the 5.16-MeV peak in Fig. 2(C), the number of random counts contributing to the 4.77-MeV peak is calculated to be 24. In the 3-h random-coincidence run mentioned above, 2 counts were observed in the 4.77-MeV peak, a number that is consistent with the calculated total of 24 in 40 h. After subtraction of the calculated random counts there remain 135 ± 17 real counts in the 4.77-MeV triple-coincidence peak. Thus, in this α-RC-γ triple-coincidence run the net intensity ratio of the alpha-particle lines populating the 4.77- and the 5.16-MeV states is $(5.4\pm0.7)\times10^{-4}$. In another run taken with not quite as good statistics the corresponding ratio was $(4.4\pm0.9)\times10^{-4}$. The weighted average of these results is $(5.0\pm0.6)\times10^{-4}$ for the 4.77/5.16 triple-coincidence intensity ratio. A calculation of the gamma-ray branching of the 4.77-MeV state, based on this result and on the results of the following sections is given in Sec. IIIB.

2. *Gamma-Ray and Alpha-Particle Branching of the B^{10} 5.16-MeV Level*

Relative intensities of the gamma-ray and alpha-particle emissions from the 5.16-MeV level of B^{10} were determined in two separate ways. In one experiment, the alpha particles populating the 5.16-MeV state were observed in coincidence with the corresponding B^{10} recoil nuclei which follow gamma-ray emission. The coincidence rate, corrected for the efficiency of detecting the recoils, was compared with the alpha-particle singles rate in order to derive the branching. In the other experiment the populating alpha particles were observed at 90° in coincidence with decay alpha particles entering a second detector, excluding B^{10} recoil nuclei from the latter detector with an absorber foil. The alpha-particle branch from the 5.16-MeV level was found by comparing this yield with the corresponding coincidence yield due to the 5.11-MeV level of B^{10}.

a. Alpha-recoil coincidence measurements. The sharp kinematic angular correlation between the alpha particles and B^{10} recoil nuclei in the $B^{11}(He^3,\alpha)B^{10}$ reaction may be used in the determination of the fractional gamma-ray decay of states in B^{10}. Since a B^{10} recoil nucleus can occur only if a state decays by gamma-ray emission to the ground state of B^{10} the fractional gamma-ray decay is given by the ratio,

$$\Gamma_\gamma/\Gamma=[(\alpha\text{-RC})_{\text{coin.}}/\epsilon_{\text{RC}}]/\alpha, \qquad (1)$$

where $(\alpha\text{-RC})_{\text{coin.}}$ is the alpha-recoil coincidence rate, α is the singles rate of populating alpha particles, and ϵ_{RC} is the efficiency for detecting the B^{10} recoil nuclei. If it is assumed that the alpha-gamma angular correlation is isotropic and that the recoil momentum imparted by the gamma rays at 90° to the reaction plane has a negligible influence on the detection efficiency, the recoil efficiency can be expressed as,

$$\epsilon_{\text{RC}}=(\alpha\text{-RC-}\gamma)_{\text{coin.}}/(\alpha\text{-}\gamma)_{\text{coin.}}, \qquad (2)$$

where $(\alpha\text{-RC-}\gamma)_{\text{coin.}}$ is the alpha-recoil-gamma triple-coincidence rate. Experimental tests, described below, were carried out to examine the influence of such correlation and recoil effects, and the results of these tests showed that in the present configuration these effects had no observable influence on the recoil efficiency. If the measurements of the two coincidence rates in Eq. (2) are made simultaneously, using the same pulse-height bias channel on the gamma rays, the gamma-ray detection efficiency cancels out exactly.

Hence, to determine the recoil detector efficiency, pulse-height windows were placed on both the 5.16-MeV alpha-particle line and the 5.16-MeV recoil peak; the NaI(Tl) gamma-ray detector was biased to accept pulses above 0.6 MeV; and simultaneous measurements were made of the alpha-recoil-gamma triple-coincidence rate and of the alpha-gamma double-coincidence rate. In each case, random-coincidence rates were also measured and subtracted from the corresponding totals. As a check on these procedures and for the purpose of normalization similar measurements were carried out on the 3.59-MeV level of B^{10} which can decay only by gamma-ray emission, i.e., $(\Gamma_\gamma/\Gamma)_{3.59}\equiv 1.00$.

In the final arrangement that was adopted, four scalers recorded the (α-RC-γ) and (α-γ) coincidence rates for the 5.16- and 3.59-MeV lines, and two 400-channel pulse-height analyzers were used in the split-memory mode simultaneously as four 200-channel analyzers. One analyzer stored the output of the recoil detector in coincidence with channels (1) on the 5.16-MeV alpha-particle line and (2) on the 3.59-MeV alpha-particle line. The second analyzer monitored the output of the alpha-particle detector contained within the windows placed (1) on the 5.16-MeV alpha-particle line and (2) on the 3.59-MeV alpha-particle line. Random coincidences were subtracted from the recoil spectra stored in the analyzer, and in the case of the 5.16-MeV recoil peak [see Fig. 4(A)] the estimated real contribution under this peak due to alpha and Li^6 breakup particles was also subtracted. The (α-RC) coincidence rates were then obtained from the net areas under the recoil peaks stored in the analyzer. By recording data with the split-memory technique the dead-time losses in the analyzer are the same for both of the recoil-coincidence spectra. In the final analyses values for $(\Gamma_\gamma/\Gamma)_{5.16}$ were derived by normalizing the 5.16-MeV data to a value of $\Gamma_\gamma/\Gamma\equiv 1.00$ for the 3.59-MeV level. If for any reason the experimental value of Γ_γ/Γ for the 3.59-MeV level turns out to differ slightly from unity, the value of Γ_γ/Γ for the 5.16-MeV level can be corrected accordingly.

A series of measurements were made at two recoil angles, 53° and 54°, between the maxima of Fig. 3 but favoring the 3.59-MeV line for reasons of statistical accuracy. At $\theta_{RC}=53°$ the recoil detection efficiencies calculated by the use of Eq. (2) were 0.48 for the 5.16-MeV line and 0.74 for the 3.59-MeV line whereas the corresponding efficiencies at $\theta_{RC}=54°$ were 0.27 and 0.78, respectively. The measured values of Γ_γ/Γ for the 3.59-MeV line, calculated according to Eq. (1) were generally within 5% of unity.

Because of the possible α-γ angular correlation and gamma-ray recoil effects, a second set of measurements was carried out after halving the distance of the recoil detector from the target without changing the 1.5×9-mm^2 detector slit. In this case, runs were made at recoil-detector angles of 50.5°, 51.5°, and 52.5°. The measured recoil-detection efficiency for each of the two lines was greater than 0.85 at each of the three angles. Again, in this series of measurements, the measured values of $(\Gamma_\gamma/\Gamma)_{3.59}$ were generally within 5% of unity.

The results of both series of runs described above agreed within their errors of ±5% despite a factor of 4 difference in the acceptance solid angle of the recoil detector and a factor of 3 variation in the recoil-detection efficiency for the 5.16-MeV level. This indicates that even in the first series of runs taken in the better geometry the uncertainties due to α-γ correlation and gamma-ray recoil effects are small.

Further confidence in the data may be obtained by comparing the measured and calculated effective gamma-ray efficiencies ϵ_γ for the decays of the 5.16- and 3.59-MeV levels. The measured ratio of gamma-ray efficiencies is given by the relationship,

$$\frac{\epsilon_{\gamma(5.16)}}{\epsilon_{\gamma(3.59)}}=\frac{(\alpha-\mathrm{RC}-\gamma)_{5.16}/(\alpha-\mathrm{RC})_{5.16}}{(\alpha-\mathrm{RC}-\gamma)_{3.59}/(\alpha-\mathrm{RC})_{3.59}}. \quad (3)$$

Experimental values for this ratio were derived from the data of the first set of measurements. The average of the various runs was $\epsilon_{\gamma(5.16)}/\epsilon_{\gamma(3.59)}=1.20\pm0.05$. This is to be compared with calculations of the expected efficiency ratio based on the accepted gamma-ray decay schemes[9,10] of the 5.16- and 3.59-MeV levels together with the tabulated gamma-ray efficiencies[11] for a 5×5-in NaI crystal. Straightforward procedures allowed for gamma-ray summing, the bias energy of 0.6 MeV, and the source-to-crystal distance of 2.0 cm. The result for isotropic α-γ correlations is $\epsilon_{\gamma(5.16)}/\epsilon_{\gamma(3.59)}$(calc.) $=1.22\pm0.06$ where most of the error comes from the uncertainties in the gamma-ray branching ratios of the two levels. The excellent agreement between the calculated and measured efficiency ratios again suggests that the effects of (α-γ) correlations on the (α-RC) efficiency measurements described earlier are small.

As described above, the data were used to obtain values for the (α-RC) coincidence rates corrected for recoil efficiency. Based on the results of the two separate runs described above, the weighted average value,

$$\frac{(\alpha-\mathrm{RC})_{5.16}/\epsilon_{\mathrm{RC}(5.16)}}{(\alpha-\mathrm{RC})_{3.59}/\epsilon_{\mathrm{RC}(3.59)}}=4.12\pm0.16,$$

is obtained. A calculation of $(\Gamma_\gamma/\Gamma)_{5.16}$ making use of this result and the results of the following sections is presented in Sec. IIIA.

b. Alpha-alpha coincidence measurements. For a state such as the 5.16-MeV level of B^{10} that decays predominantly by gamma-ray emission, the detection of the

[10] F. Ajzenberg-Selove and T. Lauritsen, Nucl. Phys. **11**, 1 (1959).

[11] S. H. Vegors, L. L. Marsden, and R. L. Heath, Phillips Petroleum Report IDO 16370, 1958 (unpublished).

alpha-particle branch is inherently more sensitive and indeed more convincing if the decay alpha particles are observed directly. In the present case, the 5.11-MeV level can serve as a useful reference since this state has a width of 1.2 keV[10] and is known to decay very nearly 100% by alpha-particle emission. Because of the close proximity of the 5.16- and 5.11-MeV levels the kinematically allowed angles for alpha-particle emission from these two states are almost the same, and thus the efficiencies for detecting alpha particles in large-solid-angle geometry should be nearly equal except for possible angular correlation effects. On the other hand, the closeness of these states means that the coincidence effects can be separated only if the resolution for detecting the populating alpha particles is adequate.

In order to obtain a resolution substantially better than that of Fig. 2(A) a number of steps were taken. A 2-mil thick ($\sim 50\,\mu$) detector, fabricated at the Bell Telephone Laboratories, was used for detecting the populating alpha particles at 90° to the beam. Line broadening due to electronic noise was minimized by the use of a special low-noise preamplifier feeding a Cosmic Radiation Company model 901 amplifier operated with single delay-line clipping. The over-all electronic linewidth (full width at half-maximum) as measured with a pulser was 20 keV when the detector was connected and biased for operation. For recording the spectra a 1024-channel section of a TMC 16 384-channel pulse-height analyzer was used. A compromise was made between the coincidence yield and the kinematic line broadening (38 keV per degree at 90° for the 5.16-MeV alphas when $E_{He^3}=3.50$ MeV) by placing the detector behind a 1-mm wide slit at a distance of 5.0 cm from the target (total slit width 1.1°). The beam was collimated to a diameter of 1 mm and the target was positioned for transmission geometry in order to mimimize the line broadening due to the 50 μ g/cm^2 target thickness. It was calculated that the rate-of-energy loss of a 3.5-MeV incident He^3 beam is very nearly equal to the rate-of-energy loss of the 4.57-MeV alpha particles populating the 5.16-MeV state. Thus in transmission geometry with a target angle of 45° there should be very little line broadening due to the target thickness. However, for the reasons outlined below the target could not quite be placed at this most favorable angle in the coincidence measurements.

Figure 5(A) shows the alpha-particle singles spectrum at −90° taken with the detector slit as described above and with the normal of the target at −45° to the beam. A comparison of these data with those in Fig. 2(A) demonstrates the improvement in resolution that has been achieved. The linewidth of 44 keV for the 4.77-MeV peak in Fig. 5(A) is approximately that expected from the combined effects of kinematic broadening and electronic noise.

Values reported[10] for the energies of the 5.11- and 5.16-MeV levels of B^{10} are 5.105 and 5.159 MeV.

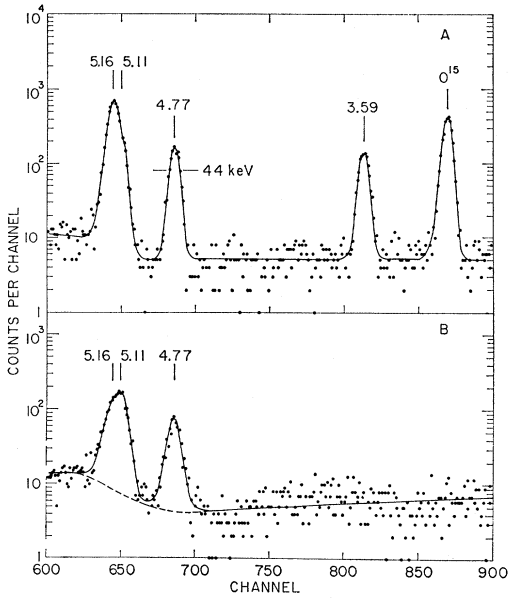

FIG. 5. (A) Curve of alpha-particle singles spectrum from the $B^{11}(He^3,\alpha)B^{10}$ reaction observed at −90° and with $E_{He^3}=3.50$ MeV. The slit in front of the detector was 1.0×6 mm^2 at a distance of 5.0 cm from the target. (B) Curve of alpha-particle spectrum in coincidence with decay alpha particles (0.028 μA for 21 h). The second detector had a 9-mm-diam aperture 2.0 cm from the target spot. It was centered at +55° to the beam, and a 1-mg/cm^2-thick Ni foil covered the detector to exclude B^{10} recoil nuclei.

Although the errors in both absolute values are quoted as ±7 keV it is very probable that the 54-keV separation between the levels is accurate to 5 keV or less. Under the conditions of the present experiment the calculated energy separation of the two alpha-particle lines is then 39 keV. This is less than the experimental linewidth for the 4.77-MeV peak, but the presence of the 5.11-MeV line is clearly seen in Fig. 5(A) as a bump on the high-energy side of the 5.16-MeV line. The positions of the 5.16- and 5.11-MeV peaks in Fig. 5(A) have been indicated with a separation of 39 keV.

Kinematic calculations served as a guide to setting up the coincidence experiments. For both the 5.16- and 5.11-MeV states the decay alpha particles which are emitted in coincidence with populating alpha particles observed at −90° must lie within a cone centered at +53° (the same angle as for B^{10} recoil nuclei following gamma-ray decay) with a half-angle of about 35°. The energies of the alpha particles are double-valued corresponding to motion towards or away from the detector in the center-of-mass system.

For one series of runs the solid-state detector for the decay alpha particles was positioned at +55° to the beam and at a distance of 2.0 cm from the target. A circular tantalum aperture 9 mm in diameter (half-angle 13°) and a nickel foil 1 mg/cm^2 thick were placed in front of the detector. The degradation of the alpha-particle energies by the foil was estimated to be ~1 MeV but it was expected that the foil would remove

completely the B^{10} recoil nuclei. In order to prevent this detector from being partly obscured by the target frame the angle of the target normal was set at $-52°$ with respect to the beam. This was expected to make the resolution somewhat poorer than in Fig. 5(A).

Figure 5(B) shows the spectrum of populating alpha particles at $-90°$ in coincidence with the alpha-particle detector at $+55°$ when the pulse-height bias on the latter was set to accept all pulses above the electronic noise. The 4.77-MeV peak in Fig. 5(B) has the same position within one channel as in Fig. 5(A) but it is somewhat broader. Although the greater width may be partly the result of the less favorable target angle it is believed that small shifts of the electronic gain during this run were responsible for the poorer resolution. The expected positions of the 5.16- and 5.11-MeV lines are indicated in Fig. 5(B) at the same channel numbers as in Fig. 5(A). It may be noted in Fig. 5(B) that the 3.59-MeV peak and the O^{15} line are both missing indicating that the random-coincidence contribution is negligible and that the B^{10} recoil nuclei corresponding to the 3.59-MeV level are removed completely by the absorber foil. Since the energy of the B^{10} recoils corresponding to the 3.59-MeV level is higher than for the recoils corresponding to any state in B^{10} above 3.59 MeV, then it is certain that the peaks in Fig. 5(B) must be due to the detection of decay alpha particles(and possibly Li^6 particles) in coincidence with the populating alpha particles. It is evident from Fig. 5(B) that the 5.16- and 5.11-MeV components are both present and that the 5.11-MeV peak is the stronger of the two.

Because of the possible effects of α-α angular correlation on the relative coincidence yields of the 5.16- and 5.11-MeV lines, another set of data was taken after moving the decay-alpha detector in to 1.0 cm from the target with no change in the aperture (half-angle 24°) and centering it at $+67°$ to the beam. The resulting spectrum had essentially the same shape as that in Fig. 5(B).

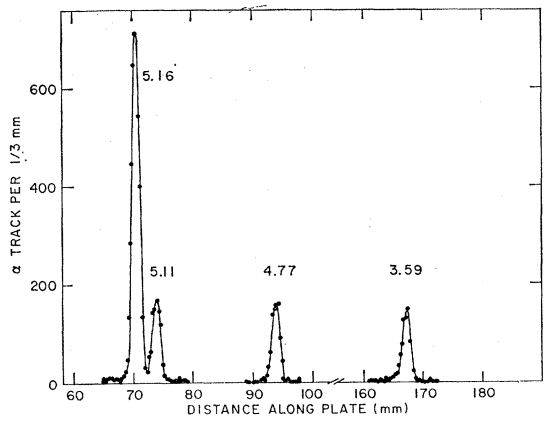

FIG. 6. Alpha-particle spectrum from the $B^{11}(He^3,\alpha)B^{10}$ reaction at $\theta=90°$ and $E_{He^3}=3.50$ MeV measured by means of a Buechner-type broad-range magnetic spectrograph.

The analysis of the relative intensities of the 5.16- and 5.11-MeV alpha-particle lines in coincidence with decay alpha particles was made by using the shape of the net 4.77-MeV line as a reference. In the singles spectrum of Fig. 5(A) the shapes and widths of the 4.77- and 3.59-MeV lines are so nearly the same that it is safe to assume that the shape of a single line should change very little between the 4.77- and 5.16-MeV positions. Fits were made to the doublet by a computer program and checked by hand, assuming that only two lines are present and that they have the known separation of the 5.16- and 5.11-MeV B^{10} levels. The relative intensities of the doublet in the signals spectrum of Fig. 5(A) were analyzed with the resulting ratio $\alpha_{5.16}/\alpha_{5.11}=3.2\pm0.7$ in good agreement with the ratio from magnetic spectrograph measurements to be discussed in the next section. The ratios extracted from the two coincidence runs agree within the experimental errors for each run with an average value of $(\alpha\text{-}\alpha)_{5.11}/(\alpha\text{-}\alpha)_{5.16}=2.1\pm0.5$. The agreement between the ratios extracted from the two coincidence runs suggests that if any differences are present in the alpha-alpha angular correlations for the 5.16- and 5.11-MeV states the effects are not great enough to introduce sizeable uncertainties in the comparison of yields. An analysis of the alpha-particle branching of the 5.16-MeV level based, in part, on these experiments is given in Sec. IIIA.

3. *Relative Intensities of Alpha-Particle Lines in Singles*

Analyses of the data presented in the preceding two sections require an accurate knowledge of the relative alpha-particle line intensities in the $B^{11}(He^3,\alpha)B^{10}$ reaction. It would be desirable to obtain these numbers under precisely the same experimental conditions of beam energy, target thickness, and detector angle as used in the coincidence experiments. This can, in fact, be done for the ratios $(\alpha_{5.16}+\alpha_{5.11}):\alpha_{4.77}:\alpha_{3.59}$ by using the data of Figs. 2(A) and 5(A). From the averages of these runs together with several others the intensity ratios $(\alpha_{5.16}+\alpha_{5.11}):\alpha_{4.77}:\alpha_{3.59}=6.1:1.11:1.00$ are obtained with accuracies of $\pm3\%$.

The relative intensities of the 5.16- and 5.11-MeV groups cannot be derived with sufficient accuracy from Fig. 5(A). In order to measure these lines at a considerably better resolution a Buechner-type magnetic spectrograph was used to observe the singles spectrum at $\theta=90°$ and $E_{He^3}=3.5$ MeV. The target consisted of a 10 μ g/cm^2 thick layer of B^{11} evaporated onto a thick Ta backing. Figure 6 shows the spectrum obtained. Four individual readings of the plates were made and the average ratio 5.16/5.11=3.32 was obtained with an error of $\sim3\%$. It should be pointed out that the ratio (5.16+5.11)/3.59 derived from the data of Fig. 6 is about 10% lower than the results from the solid-state-detector data cited above. This difference is more than twice the sum of the errors of the individual measure-

ments and the reason for the discrepancy is not clear. In the present analysis only the $\alpha_{5.16}/\alpha_{5.11}$ ratio was taken from the Buechner spectrograph data. Because of the proximity of these lines it was expected that systematic errors in this ratio should be small. By combining the various line intensity ratios given above the relative intensities,

$$\alpha_{5.16}:\alpha_{5.11}:\alpha_{4.77}:\alpha_{3.59}=4.70:1.42:1.11:1.00(\pm 3\%)$$

are adopted.

4. Search for Population of the 5.18-MeV State of B^{10}

Implicit in the above analysis of the singles intensities is the assumption that if the broad 5.18-MeV state of B^{10} is populated in the $B^{11}(He^3,\alpha)B^{10}$ reaction the corresponding alpha-particle line has not interfered with the extraction of the 5.16- and 5.11-MeV line intensities. In neither Fig. 5(A) nor Fig. 6 is there any evidence for a broad alpha-particle line corresponding to this state. As a further check a run was made with the Buechner spectrograph at $\theta=90°$ and $E_{He^3}=3.5$ MeV at an effective resolution of 60 keV with a resulting spectrum very similar in appearance to that in Fig. 5(A). An upper limit to the intensity of a 5.18-MeV line can be derived after assuming a value for its width in the laboratory system. Two published measurements give values of about 200 keV[12] and about 100 keV[13] for the center-of-mass width of the 5.18-MeV state. For purposes of argument we assume that the laboratory width of the populating alpha-particle group at $\theta=90°$ and $E_{He^3}=3.5$ MeV is 150 keV. By means of curve construction the contribution of such a line to the doublet in Fig. 5(A) is estimated to be $<6\%$ of the area under the (5.16+5.11)-MeV doublet. Furthermore, since not all of the line would lie within the bounds of the 5.16-5.11-MeV doublet the maximum contribution to the area of the doublet would be $\sim 4\%$, and this may be considered as an upper limit to a possible additional error. Should the width of the 5.18-MeV line be smaller than 150 keV the error in the (5.16+5.11)-MeV doublet would be larger, but then one might expect to see the 5.18-MeV line in the data of Fig. 6 where the effective resolution is 25 keV. On the other hand, a line wider than 150 keV would give a smaller error since it would tend to blend into the background and be subtracted out as part of the background. We conclude that if the 5.18-MeV state of B^{10} is populated its intensity under our experimental conditions is too small, regardless of the width of the line, to affect the results of the various experiments described above.

B. The $Li^6(\alpha,\gamma)B^{10}$ Reaction

Investigations of the gamma radiation emitted in the decay of the 4.77- and 5.16-MeV levels of B^{10} were made by exciting these states in the $Li^6(\alpha,\gamma)B^{10}$ reaction at the known $E_{He^4}=0.500$-MeV and $E_{He^4}=1.175$-MeV resonances. Thick targets of Li^6F or evaporated Li^6 metal were used in the various experiments. In the Lockheed experiments the Li^6 was evaporated *in situ* onto a target "wobbler" which was cooled externally with a water spray. The He^{4+} beam energy was generally set about 50 keV above the resonant energy so that the resonance region was slightly below the target surface. Most of the measurements were made using a 5×5-in. NaI crystal having a pulse-height resolution of 9.2% for the 0.662-MeV gamma rays of Cs^{137}. Conventional amplifiers and pulse-height analyzers were employed.

An important consideration in all of this work was the background counting rate in the NaI crystal in the pulse-height region from 3 to 6 MeV. Two types of background were observed in this region: (1) prompt radiations associated with beam acceleration and (2) activities (mostly 15-h Na^{24}) induced in the crystal by neutrons. In the early stages of experiments at Brookhaven, relatively high backgrounds of both types appear to have been caused by D^+, HD^+, or D_2^+ beam components producing neutrons and prompt gamma rays in various parts of the beam transport system or even in the Li target itself. After several weeks of operation the residual deuterium gradually cooked out of the ion source and the background level in the region between 5 and 6 MeV fell to a level which was essentially the same when the beam was on target as it was with the machine completely off.

In the Van de Graaff accelerator at Lockheed the gas manifold system in the terminal was reconstructed and a fresh rf ion-source bottle installed just before the experiments were begun in order to avoid any repetition of the problems initially encountered at Brookhaven due to deuteron components in the beam. With a 35-μA He^4 beam on a Li^6 target the counting rate in the 5–6-MeV region was essentially the "natural" room background.

1. Angular Distribution of the 4.05-MeV Gamma Radiation from the 4.77-MeV Level

Conventional techniques were used in measuring the angular distribution of the 4.05-MeV gamma rays from the 4.77-MeV level in B^{10} formed by the $Li^6(\alpha,\gamma)B^{10}$ reaction at the $E_{He^4}=0.50$-MeV resonance. The 5×5-in. NaI crystal was placed on the angular distribution table at a target-to-crystal distance of 20.0 cm. The net yield under the 4.50-MeV full-energy-loss peak was plotted versus the detector angle with the results shown in Fig. 7. A computer fit to the data points (solid line in Fig. 7) was carried out in order to determine the experimental A_2 and A_4 coefficients. These coefficients were then corrected for the finite solid angle of the detector by using the tables of Gove and Rutledge.[14] The

[12] E. L. Sprenkel, J. W. Olness, and R. E. Segel, Phys. Rev. Letters **7**, 174 (1961).

[13] G. Dearnaley, D. S. Gemmell, and S. S. Hanna, Nucl. Phys. 36, 71 (1962).

[14] H. E. Gove and A. R. Rutledge, Atomic Energy of Canada Report AECL-1449, 1958 (unpublished).

corrected angular distribution expressed in terms of the Legendre polynomials P_2 and P_4 is given by,

$$W(\theta)_{4.05\gamma}=1+(0.510\pm0.024)P_2(\cos\theta) - (0.295\pm0.030)P_4(\cos\theta). \quad (4)$$

In Fig. 8 the measured value of $A_2=(0.510\pm0.024)$ is compared to the theoretical values for $J^\pi=3^+\rightarrow J^\pi=1^+$ and for $J^\pi=2^+\rightarrow J^\pi=1^+$ transitions using $l=2$ alpha-particle capture only. From a similar comparison of the theoretical and experimental values of A_4, one also obtains $\tan^{-1}\delta\approx0°(3^+)$, $\approx40°(2^+)$. (See Fig. 8 caption for the definition of δ.) The angular distribution of the 4.05-MeV gamma rays is therefore consistent with either a $J^\pi=2^+$ or 3^+ assignment for the 4.77-MeV level. These experimental results disagree with those of Meyer-Schützmeister and Hanna[6] who concluded that $J^\pi=3^+$ was possible only for an inadmissible $l_\alpha=4$ to $l_\alpha=2$ intensity ratio of order unity. Our distribution is in essential agreement with that of Warhanek[7] who finds $J^\pi=3^+$.

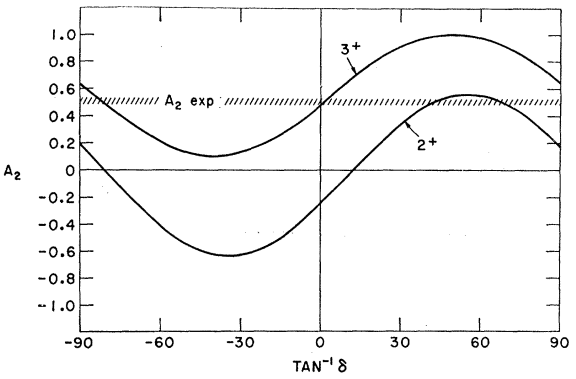

FIG. 8. Theoretical plots of the angular distribution coefficient A_2 versus $\tan^{-1}\delta$ (where δ is the $E2/M1$ amplitude ratio for the 2^+ curve and the $M3/E2$ amplitude ratio for the 3^+ curve) for the 4.05-MeV gamma rays from the 4.77-MeV state formed at the 0.500-MeV resonance in the $Li^6(\alpha,\gamma)B^{10}$ reaction. The shaded region is allowed by the experimental result, $A_2=0.510\pm0.024$ ($l_\alpha=2$ only is used for the theoretical curves).

2. *4.05-0.72-MeV Gamma-Gamma Angular Correlation from the 4.77-MeV Level*

For these measurements, two 5×5-in. NaI detectors were each placed 12.2 cm from the target. One detector was fixed at −90° to the beam and the other was varied from 0° to +90° with respect to the beam. A window, 3.22 MeV$\leq E_\gamma\leq$4.55 MeV, was placed around the full-energy peak in the spectrum of the 4.05-MeV gamma ray in the output of the fixed detector. The coincident spectra of the 0.72-MeV gamma radiation in the moving crystal were recorded at 7 angles from 0° to 90° in steps of 15° for charge collections of 500 μC each. In the one set of runs that was made, the experimental gamma-gamma angular correlation was found to be isotropic within the individual statistical errors of ±10%. Since the lifetime of the 0.72-MeV level of B^{10} is known[10] to be about 10^{-9} sec it is probable that gamma-gamma angular correlations involving cascades through this state would be attenuated by "loss-of-memory" effects. In view of the probable difficulty of interpreting a more accurate measurement of the 4.05-0.72-MeV gamma-gamma angular correlation, no further effort was expended on this part of the work.

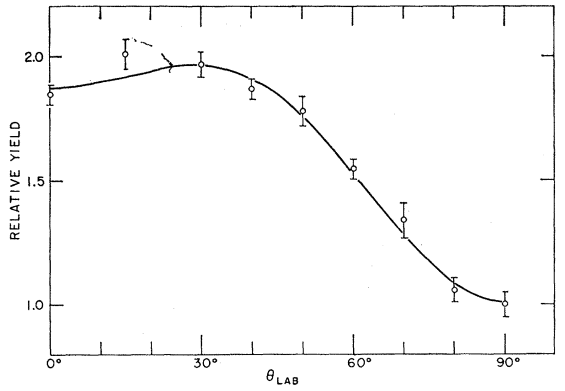

FIG. 7. Experimental angular distribution of the 4.05-MeV gamma rays occurring in the $Li^6(\alpha,\gamma)B^{10}$ reaction at the $E_{He^4}=0.50$-MeV resonance and with a target-to-crystal distance of 20.0 cm. The curve is a computer fit to the data.

3. *Intensity of the 4.77-MeV Ground-State Transition*

During the experiments described above studying the decay of the 4.77-MeV level in B^{10} by the emission of a 4.05-MeV gamma ray to the 0.72-MeV first excited state of B^{10}, it was observed that the decay of this level directly to the ground state by the emission of a 4.77-MeV gamma ray must have a relative intensity of <1%. In order to detect and measure such a weak line, it is necessary to obtain as high a reaction yield as possible while at the same time minimizing the summing effect of the 4.05- and 0.72-MeV gamma rays in the detector. The best reaction yield that could be achieved was obtained by using a thick Li^6 metallic target bombarded with a 0.55-MeV He^{4+} beam of 35 μA.

If no absorber is used the ratio of the (4.05+0.72)-MeV summing-line photopeak intensity relative to the 4.05-MeV photopeak intensity is simply the photopeak efficiency for the 0.72-MeV gamma rays, i.e., 1.1% at a detector distance of 20 cm. Relative summing contributions can, of course, be reduced by increasing the target-to-crystal distance, with the consequent reduction in detector solid angle. However, since the absorption cross section of a material such as lead is much higher for a 0.72-MeV gamma ray than it is for a 4.77-MeV gamma ray, in the present case the use of an absorber is a much more efficient way to reduce the summing contribution relative to the 4.77-MeV transition. For example, by moving the detector from 20 cm to 50 cm the intensity of 4.77-MeV gamma radiation incident on the crystal is reduced by a factor of 4.5,

while the (4.05+0.72)-MeV summing intensity is reduced by a factor of $(4.5)^2$ for a relative reduction of 4.5 from 1.1 to 0.2%. However, if a lead absorber 3.2 cm thick is placed in front of the 5×5-in crystal while it is 20 cm from the target, the intensity of 4.77-MeV radiation is again reduced by a factor of 4.5, but the summing intensity is reduced by a factor of 165 for a relative reduction of 36 from 1.1 to 0.03%.

In the final experiments the 5×5-in. NaI crystal was placed 20.0 cm from the target and at 0° to the beam. The crystal was enclosed by a 2-in. thick cylindrical Pb shield and five $\frac{1}{4}$-in. thick Pb plates were stacked immediately in front of the detector. The pulse-height spectrum from runs totaling 26 h at a beam current of 28–30 μA revealed the presence of a 4.77-MeV photopeak, whose intensity was found to be (0.53±0.10)% as strong as the 4.05-MeV photopeak after making a small correction for the difference between the 4.05- and 4.77-MeV photopeak efficiencies. By subtracting the summing contribution of 0.03%, as explained above, the value (0.5±0.1)% is found for the 4.77/4.05 intensity ratio at 0°. As will be seen in the next section, the angular distributions of the 4.77- and 4.05-MeV gamma rays are so nearly similar that the value (0.5±0.1)% may be taken as the relative ground-state branching intensity. This result disagrees sharply with that of Meyer-Schützmeister and Hanna[6] who found a ground-state branch of 8% but is consistent with the 3% upper limit of Warhanek.[7]

4. *Angular Distribution of the 4.77-MeV Gamma Radiation*

In order to obtain a higher counting rate for angular distribution measurements on the 4.77-MeV gamma rays the 5×5-in. crystal was moved in to a distance of 11.0 cm from the target without changing the Pb shield and absorbers. Under these conditions, the calculated (4.05+0.72)-MeV summing line was 0.077%

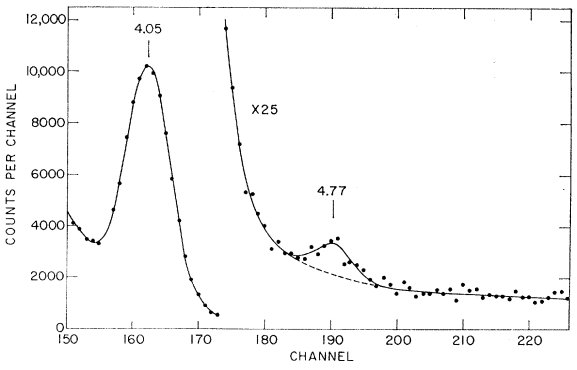

FIG. 9. Pulse-height spectrum obtained in one of the 6-h runs at 0° on the angular distribution of the 4.77-MeV gamma-rays in the $Li^6(\alpha,\gamma)B^{10}$ reaction at the $E_{He^4}=0.50$-MeV resonance. At the 11.0-cm target-to-crystal distance and with the lead absorber used the (4.05+0.72)-MeV summing contribution was 15% of the total 4.77-MeV photopeak.

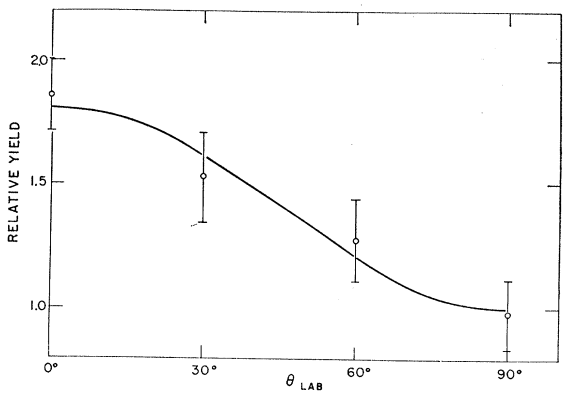

FIG. 10. Experimental angular distribution of the 4.77-MeV gamma rays occurring in the $Li^6(\alpha,\gamma)B^{10}$ reaction at the $E_{He^4}=0.50$-MeV resonance. The curve is a computer fit to the data.

as strong as the 4.05-MeV line or about 15% relative to the real 4.77-MeV line. Spectra were recorded at 4 angles between 0° and 90° with a total of 12 h of running at each angle. One of the 6-h runs is shown in Fig. 9. The net area under the 4.77-MeV line in each of the runs was extracted by means of a computer curve-fitting program, and from this area the calculated summing contribution was subtracted.

The general procedure for finding the angular distribution of the 4.77-MeV gamma rays was to use the 4.77/4.05 intensity ratios at the various angles together with the 4.05-MeV angular distribution for purposes of normalization. The expected 4.05-MeV gamma-ray angular distribution at a target-to-crystal distance of 11.0 cm was derived from the "true" distribution given in paragraph (1) of this section by applying to the A_2 and A_4 coefficients the appropriate attenuation factors from the tables of Gove and Rutledge.[14] By using this "constructed" 4.05-MeV angular distribution for normalization, the measured 4.77/4.05 ratios give the experimental angular distribution for the 4.77-MeV gamma rays shown in Fig. 10. A computer fit to the data points by the method of least squares was made (solid curve in Fig. 10) and the experimental coefficients $A_2=(0.38\pm0.12)$ and $A_4=(0.05\pm0.14)$ were obtained. These coefficients were then corrected for geometry with the final result that the corrected angular distribution for the 4.77-MeV gamma rays is given by,

$$W(\theta)_{4.77\gamma}=1+(0.44\pm0.14)P_2(\cos\theta)+(0.09\pm0.23)P_4(\cos\theta). \quad (5)$$

The theoretical values of A_2 for $3^+\rightarrow 3^+$ and for $2^+\rightarrow 3^+$ transitions are compared in Fig. 11 to the measured value of 0.44±0.14, indicating an assignment of $J^\pi=3^+$ for the 4.77-MeV level. The value of A_4 is consistent with this assignment. A more accurate measurement of this angular distribution would be desirable.

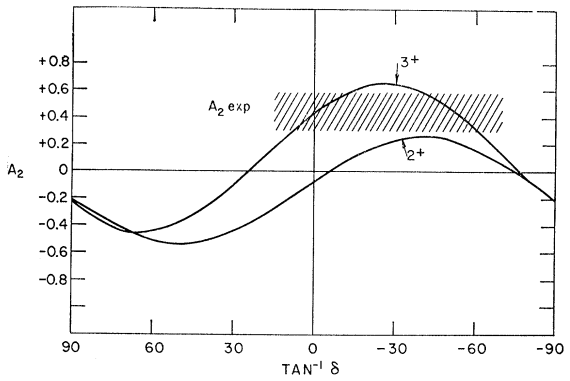

FIG. 11. Theoretical plots of the angular distribution coefficients A_2 versus $\tan^{-1}\delta$ (where δ is the $E2/M1$ amplitude ratio) for the 4.77-MeV gamma rays in the $Li^6(\alpha,\gamma)B^{10}$ reaction. The two curves are for 2^+ and 3^+ assignments and the shaded region is allowed by the experimental result $A_2=0.44\pm0.14$.

5. *Thick-Target Gamma-Ray Yield at the 4.77-MeV Level*

The absolute gamma-ray width Γ_γ of the 4.77-MeV level of B^{10} was determined from measurements of the thick-target yield for the $Li^6(\alpha,\gamma)B^{10}$ reaction at the 0.500-MeV resonance. $\Gamma_\gamma\Gamma_\alpha/\Gamma$ can be expressed in terms of the thick-target yield as

$$\frac{\Gamma_\gamma\Gamma_\alpha}{\Gamma}=\frac{(2S_0+1)(2S_1+1)}{(2J+1)}\frac{2\epsilon}{\lambda_{c.m.}^2}y, \tag{6}$$

where S_0, S_1, and J are the spins of the target nucleus, the incident projectile, and the resonant state, respectively; ϵ is the stopping cross section of alpha particles per LiF molecule at the resonance energy; $\lambda_{c.m.}$ is the wavelength of the projectile in the center of mass $=[(M_1+M_0)/M_1]\{h/[2M_1E_1(\text{lab})]^{1/2}\}$; y is the thick-target yield of gamma rays per incident particle. In the present case $S_0=1$, $S_1=0$ and for 0.500-MeV alpha particles $\lambda_{c.m.}=3.9\times10^{-12}$ cm. LiF enriched to 96% Li^6 was used for the target so that[15]

$$\epsilon=(23.3+47.7)\frac{1}{0.96}\times10^{-15}\text{ eV cm}^2 \tag{7}$$
$$=(74\pm12)\times10^{-15}\text{ eV cm}^2,$$

where 23.3×10^{-15} eV cm^2 and 47.7×10^{-15} eV cm^2 are the stopping cross sections for 0.500-MeV alpha particles in lithium and fluorine, respectively, and where the factor $(0.96)^{-1}$ arises from the 96% Li^6 abundance in the target.

Considerable attention was paid to the measurement of the integrated beam current in order to ensure that secondary electrons were not causing spurious readings: In the final measurements the target was biased to +300V and was shielded electrostatically and magnetically against secondary electrons from the beam collimators and control slits. In order to test the possibility that the He^{4+} beam might have been contaminated with a He^{4++} component resulting from stripping in the residual gas between the analyzing magnet and the target, the thick-target gamma-ray yield was measured at several energies from 550- to 800-keV. Over this range no appreciable change was observed and it was concluded that the He^{4++} component in the beam at 550 keV was probably negligible.

Gamma rays were detected using the 5×5-in NaI(Tl) crystal. In order to convert the measured full-energy peak yield to the total yield, corrections were made for analyzer deadtime (1.6%) and 4.05-MeV gamma-ray attenuation by the target backing, target chamber, and crystal housing (3.0%). Measurements were made in two different geometries, with the crystal at 0° with respect to the beam and 9 cm from the target and with the crystal at 0° with respect to the beam and 5 cm from the target. For these geometries the total efficiencies for detecting 4.05-MeV gamma rays, with the angular distribution measured in Sec. IIB1, were calculated directly, using the cross-section tables of Grodstein,[16] to be 0.056 and 0.111, respectively. The fraction of 4.05-MeV gamma rays interacting with the crystal which gives rise to counts in the full-energy peak of the spectrum was determined to be 0.262 by an interpolation from measurements made on gamma rays with energies of 0.662 MeV [Cs^{137}], 3.09 MeV [$C^{12}(d,p)C^{13}$], and 4.43 MeV [$N^{15}(p,\alpha)C^{12}$] using the method of Zerby and Moran.[17] These measurements of peak-to-total ratios are in good agreement with independent measurements on 5×5-in. NaI(Tl) crystals by Young *et al.*,[18] and by Olness.[19] A calculation using the line shapes for 0.72- and 4.05-MeV gamma rays showed that the net effect to the full-energy peak from additions and subtractions caused by summing events, where both the 0.72- and 4.05-MeV gamma rays are detected in the crystal, was only −0.13%, and this effect has therefore been neglected.

Combining all the calculations and corrections of the previous paragraph, y, the thick-target yield per incident alpha particle, was determined to be 6.05×10^{-12} for the two cases measured. Since this transition represents 99.5% of the gamma-ray decays from the 4.77-MeV level, we may combine this yield with Eq. (6) and find that for this level,

$$(\Gamma_\gamma\Gamma_\alpha/\Gamma)_{4.77}=0.033\pm0.006\text{ eV }(J^\pi=3^+),$$

where the bulk of the error lies in uncertainties in the

[15] W. Whaling, *Handbuch der Physik*, edited by S. Flügge (Springer-Verlag, Berlin, 1958), Vol. 34, p. 193. D. Demirlioglu and W. Whaling, California Institute of Technology Report, 1962 (unpublished).

[16] G. W. Grodstein, Natl. Bur. Std. (U. S.) Circ. 583, 1957.

[17] C. D. Zerby and H. S. Moran, Nucl. Instr. Methods **14**, 115 (1961).

[18] F. C. Young, H. T. Heaton, G. W. Phillips, P. Forsyth, and J. B. Marion, Bull. Am. Phys. Soc. **10**, 54 (1965).

[19] J. W. Olness (private communication).

stopping cross section for alpha particles of this low energy in fluorine. This agrees adequately with the value 0.021 ± 0.01 eV given by Warhanek.[7]

6. Thick-Target Gamma-Ray Yield at the 5.16-MeV Level

Using the same techniques described in Sec. IIB5 the step in the thick-target excitation function was measured at the 1.175-MeV resonance in the $Li^6(\alpha,\gamma)B^{10}$ reaction, corresponding to the 5.16-MeV level in B^{10}.

Our measurements were made on the 3.01-MeV transition from the 5.16-MeV level to the 2.15-MeV level. Although a thick target was used and so we were also populating the 5.11-MeV level as well, the gamma-ray yield from this level is low relative to that from the 5.16-MeV level and the transition is almost entirely to the ground state[6]; therefore no correction was necessary on this account. By using an angular distribution[6] for the 3.01-MeV gamma rays of $(1-0.25\cos^2\theta)$ and by using an analysis identical to that in Sec. IIB5 we find that for that particular transition,

$$\Gamma_\gamma\Gamma_\alpha/\Gamma=0.25\pm0.05 \text{ eV}.$$

Allowing for the fact that this transition represents $(65\pm2)\%$ [9] of the gamma transitions from the 5.16-MeV state, we find that for the 5.16-MeV state.

$$(\Gamma_\gamma\Gamma_\alpha/\Gamma)_{5.16}=0.38\pm0.08 \text{ eV}.$$

This corresponds to $\omega\gamma=0.63\pm0.13$ eV, in good agreement with the value of 0.51 ± 0.10 eV obtained by Meyer-Schützmeister and Hanna.[6]

III. PARTIAL WIDTHS OF THE 5.16- AND 4.77-MeV LEVELS

A. The 5.16-MeV Level of B^{10}

The alpha-particle and gamma-ray branching of the 5.16-MeV level may be obtained (in the first of two methods) by using the alpha-recoil coincidence results presented in Sec. IIA2a and the alpha-particle singles data given in Sec. IIA3 together with the relationship,

$$(\Gamma_\gamma/\Gamma)_{5.16}=\left[\frac{(\alpha-\mathrm{RC})_{5.16}/\epsilon_{\mathrm{RC}(5.16)}}{(\alpha-\mathrm{RC})_{3.59}/\epsilon_{\mathrm{RC}(3.59)}}\right]\times\frac{\alpha_{3.59}}{\alpha_{5.16}}. \quad (8)$$

In Eq. (8) it is implied that $(\Gamma_\gamma/\Gamma)_{3.59}\equiv1.00$ for the 3.59-MeV state. The first factor on the right-hand side of Eq. (8) is the ratio of coincidence yields for the 5.16- and 3.59-MeV states, corrected for recoil detection efficiency, and the experimental result is 4.12 ± 0.16 from Sec. IIA2a. The alpha-particle singles ratio, $\alpha_{5.16}/\alpha_{3.59}=4.70(\pm3\%)$, is taken from Sec. IIA3. By inserting these numbers into Eq. (8) the result is,

$$(\Gamma_\gamma/\Gamma)_{5.16}=0.88\pm0.04$$

and it follows that,

$$(\Gamma_\alpha/\Gamma)_{5.16}=0.12\pm0.04.$$

The second way of finding the alpha-particle branching of the 5.16-MeV state is to use the results of measurements on decay alpha particles in coincidence with the populating alpha particles as described in Sec. IIA2b. There it was shown that $(\alpha\text{-}\alpha)_{5.11}/(\alpha\text{-}\alpha)_{5.16}=2.1\pm0.5$. The alpha-particle branch may be obtained by using the relationship,

$$(\Gamma_\alpha/\Gamma)_{5.16}=\frac{(\alpha-\alpha)_{5.16}}{(\alpha-\alpha)_{5.11}}\times\frac{\alpha_{5.11}}{\alpha_{5.16}}, \quad (9)$$

where it is understood that $(\Gamma_\alpha/\Gamma)_{5.11}\cong1.00$. The alpha-particle singles ratio from Sec. IIA3 is $\alpha_{5.16}/\alpha_{5.11}=3.32(\pm3\%)$ and thus the substitution of the experimental results into Eq. (9) leads to,

$$(\Gamma_\alpha/\Gamma)_{5.16}=0.14\pm0.04.$$

By weighting equally the separate results from the two types of experiment we obtain the average value

$$(\Gamma_\alpha/\Gamma)_{5.16}=0.13\pm0.04,$$

or

$$(\Gamma_\gamma/\Gamma)_{5.16}=0.87\pm0.04.$$

The absolute partial widths may be determined by combining the above fractional branching information with the results of the thick-target yield presented in Sec. IIB6 according to which $(\Gamma_\gamma\Gamma_\alpha/\Gamma)_{5.16}=0.38\pm0.08$ eV. A simple calculation gives the partial widths,

$$\Gamma_{\gamma(5.16)}=2.9\pm1.1 \text{ eV},$$

and

$$\Gamma_{\alpha(5.16)}=0.44\pm0.09 \text{ eV}.$$

B. The 4.77-MeV Level of B^{10}

The fractional gamma-ray branching of the 4.77-MeV state, which in the present analysis depends, in part, on the value of $(\Gamma_\gamma/\Gamma)_{5.16}$, may now be derived by using the relationship,

$$(\Gamma_\gamma/\Gamma)_{4.77}=(\Gamma_\gamma/\Gamma)_{5.16}\times\frac{(\alpha-\mathrm{RC}-\gamma)_{4.77}}{(\alpha-\mathrm{RC}-\gamma)_{5.16}}\times\frac{\epsilon_{\gamma(5.16)}}{\epsilon_{\gamma(4.77)}}\times\frac{\alpha_{5.16}}{\alpha_{4.77}}. \quad (10)$$

The experiment involving alpha-recoil-gamma triple-coincidences was described in Sec. IIA1 with the result $(\alpha\text{-RC-}\gamma)_{4.77}/(\alpha\text{-RC-}\gamma)_{5.16}=(5.0\pm0.6)\times10^{-4}$. A value of 4.3 for the alpha-particle singles ratio $\alpha_{5.16}/\alpha_{4.77}$ is obtained from the data given in Sec. IIA3. The remaining factor to be determined in Eq. (10) is the gamma-ray efficiency ratio $\epsilon_{\gamma(5.16)}/\epsilon_{\gamma(4.77)}$. By using the known gamma-ray decay schemes[9,10] of the 5.16- and 4.77-MeV levels of B^{10} the relative efficiencies for a 5×5-in. NaI crystal were found in the same way as discussed in Sec. IIA2a. The calculated ratio is $\epsilon_{\gamma(5.16)}/\epsilon_{\gamma(4.77)}=1.20\pm0.06$. When all of the numbers given above are substituted into Eq. (10) the gamma-ray branching is found to be

$$(\Gamma_\gamma/\Gamma)_{4.77}=(2.3\pm0.3)\times10^{-3}.$$

TABLE II. Partial widths for the decays of the 4.77- and 5.16-MeV levels of B^{10}. The 4.77-MeV level is taken as $J^\pi=3^+$.

Level (MeV)	Γ_γ/Γ	Γ_α/Γ	$\Gamma_\alpha\Gamma_\gamma/\Gamma$ (eV)	Γ_γ (eV)	Γ_α (eV)
4.77	$(2.3\ \pm0.3)\times10^{-3}$	0.998	0.033±0.006	0.033±0.006	14±3
5.16	0.87±0.04	0.13±0.04	0.38 ±0.08	2.9±1.1	0.44±0.09

Based on an assumption of 3^+ for the spin parity of the 4.77-MeV level, it was shown from the thick-target yield data given in Sec. IIB5 that

$$(\Gamma_\gamma\Gamma_\alpha/\Gamma)_{4.77}=0.033\pm0.006\text{ eV}(J^\pi=3^+).$$

By combining this with the fractional branching derived from Eq. (10) the partial widths for gamma-ray and alpha-particle emission are (for $J^\pi=3^+$)

$$\Gamma_{\gamma(4.77)}=0.033\pm0.006\text{ eV},$$

and

$$\Gamma_{\alpha(4.77)}=14\pm3\text{ eV}.$$

If the 4.77-MeV state were 2^+ rather than 3^+ both partial widths would be larger by a factor of 5/3, i.e., $\Gamma_\gamma=0.055$ eV and $\Gamma_\alpha=23$ eV.

Data on the partial widths of the 4.77- and 5.16-MeV states are summarized in Table II.

IV. DISCUSSION

A. 4.77-MeV Level of B^{10}

1. Ground-State M1 Transition

We have shown that, for the 4.77-MeV level, $J^\pi=3^+$ is favored by the angular distribution of the weak ground-state transition. The transition to the first excited state allows $J^\pi=2^+$ or 3^+. However, for the latter assignment, already favored by the ground-state transition, the angular distribution of the transition to the first excited $J^\pi=1^+$ state is very satisfactorily fitted for the expected pure $E2$ radiation with no free parameters whereas the choice $J^\pi=2^+$ requires a particular value for the $E2/M1$ mixing ratio. The absence of the *ad hoc* parameter for the $J^\pi=3^+$ possibility is in its favor and we therefore regard $J^\pi=3^+$ as, over all, quite strongly to be preferred from our measurements. We now adopt this assignment.

As mentioned in the Introduction, IPM_{new}, unlike IPM_{old}, contains a $J^\pi=3^+$ level at just about 4.8 MeV that we may now seek to identify with our present state. A most striking experimental feature is the weak ground-state transition. We have, from the data given above, a ground-state radiative width of

$$\Gamma_{\gamma(4.77)}=(1.7\pm0.5)\times10^{-4}\text{ eV}.$$

As may be seen from Fig. 11 a considerable $E2$ component could be present in this transition although the data are compatible with pure $M1$ radiation. The data allow an $M1$ width of as little as 4×10^{-5} eV. However, even the full 1.7×10^{-4} eV, 7×10^{-5} Weisskopf units, is remarkably small even for an isotopic-spin discouraged $M1$. It is clear that nuclear structure information of importance is contained in the smallness of this width. The prediction of IPM_{new} is in striking agreement with this interesting experimental inhibition: Theoretically, the $M1$ width is about 6×10^{-6} eV.[5,20] This contrasts favorably with the prediction of IPM_{old} namely an $M1$ width of 4.8×10^{-2} eV which is much too large.

The position and the unusual weakness of the $M1$ ground-state decay of the $J^\pi=3^+$ state are therefore both most satisfactorily accounted for by IPM_{new} where IPM_{old} failed. (We may note that the $J^\pi=2^+$ possibility offered by IPM_{new} has a theoretical ground-state $M1$ width of about 3.5×10^{-2} eV which would be most unacceptable and which makes the good performance of the model's $J^\pi=3^+$ state even more pleasing.)

There remains the question of the $E2$ component of this transition. Figure 11 shows that it lies in the range 0 to 1.3×10^{-5} eV or so. As is well known, IPM wave functions do not give a good account of $E2$ transitions. The account is often made satisfactory, however, by ascribing to the neutrons involved in the IPM wave functions an effective charge of x electronic units and to the protons a charge $1+x$ where $x\approx0.5$. This appears to give a reasonably good mock-up of the collective effects and has been found satisfactory for $E2$ transitions in $A=10$ under IPM_{old}.[21] We therefore, tentatively, may compare the experimental $E2$ strengths with the predictions of IPM_{new}, unenhanced by an effective charge factor $\Gamma_\gamma(E2)$ and enhanced $\Gamma_\gamma'(E2)$. For $T=0\rightarrow T=0$ transitions $\Gamma_\gamma'(E2)=(1+2x)^2\Gamma_\gamma(E2)$ and for $T=1\rightarrow T=0$ transitions $\Gamma_\gamma'(E2)=\Gamma_\gamma(E2)$; we shall take $x=0.5$ for purposes of presentation, so in the former case $\Gamma_\gamma'(E2)=4\Gamma_\gamma(E2)$. We also use the value $\langle r^2\rangle_p=7.9\times10^{-26}$ cm^2 adopted for an earlier discussion[21] of $E2$ transitions in $A=10$.

It does not seem likely that $\langle r^2\rangle_p$ can be greater than 10×10^{-26} cm^2 at the most so the $E2$ single-particle unit could possibly be as much as 60% larger than that used in this paper with corresponding adjustment in the comparison between the IPM and experiment. Throughout this paper we shall use $\langle r^2\rangle_p=7.9\times10^{-26}$ cm^2. The predictions of IPM_{new} for the $E2$ component of this

[20] D. Kurath (private communication).
[21] E. K. Warburton, D. E. Alburger, D. H. Wilkinson, and J. M. Soper, Phys. Rev. **129**, 2191 (1963).

transition[20] then become:

$$\text{IPM}_{\text{new}(8)}: \Gamma_\gamma(E2)=1.7\times10^{-3}\text{ eV};\quad \Gamma_\gamma'(E2)=6.6\times10^{-3}\text{ eV},$$

$$\text{IPM}_{\text{new}(6)}: \Gamma_\gamma(E2)=9.1\times10^{-4}\text{ eV};\quad \Gamma_\gamma'(E2)=3.6\times10^{-3}\text{ eV}.$$

The IPM therefore grossly overestimates the strength of the $E2$ component of this transition. We must ask if it can accommodate a much smaller value.

2. 0.72-MeV State E2 Transition

The chief radiative decay of the 4.77-MeV state is the 4.05-MeV $E2$ transition to the $J^\pi=1^+$ state at 0.72 MeV with

$$\Gamma_{\gamma(4.05)}=0.033\pm0.006\text{ eV}.$$

This transition is remarkably strong: On a conventional radius constant of 1.2 F it is 28 Weisskopf units. More realistically, we may use the value $\langle r^2\rangle_p=7.9\times10^{-26}$ cm^2 referred to above.[21] One single-particle $(1p_{3/2}\rightarrow 1p_{3/2})$ unit is then: $\Gamma_\gamma=4.1\times10^{-6}E_\gamma{}^5$ eV, where E_γ is in MeV and our present transition has a strength of 7.4 such single-particle units. This is an astonishingly strong transition. We have seen that the states that it links are both part of $(1p)^6$ on the IPM and it is rather unlikely that configuration mixing or other effects could generate so powerful an $E2$ transition unless the IPM wave functions were already favorable to such a transition. Otherwise, the disturbance to the IPM wave functions would be so great that the apparently successful prediction of the small ground-state $M1$ transition probability would become meaningless chance unless the admixtures of the wave functions responsible for the $E2$ transition were orthogonal to those of the IPM in respect of the $M1$ transition to a most unlikely degree. IPM_{new} predicts:

$$\text{IPM}_{\text{new}(8)}: \Gamma_\gamma(E2)=2.2\times10^{-3}\text{ eV};\quad \Gamma_\gamma'(E2)=8.6\times10^{-3}\text{ eV},$$

$$\text{IPM}_{\text{new}(6)}: \Gamma_\gamma(E2)=2.5\times10^{-3}\text{ eV};\quad \Gamma_\gamma'(E2)=9.8\times10^{-3}\text{ eV}.$$

We see that IPM_{new} indeed predicts that this transition should be very strong, about 0.5 single-particle units without enhancement, but that, even enhanced by the effective charge factor, it fails by a significant margin to reproduce the experimental result.

We may note that if the $J^\pi=2^+$ assignment for the 4.77-MeV state were in fact the correct one a very large $E2$ strength would still be demanded in this transition. The total radiative width would then become $\Gamma_\gamma=0.046$ eV and so with the $E2/M1$ ratio of about 0.8 by intensity required to fit the angular distribution we should have $\Gamma_\gamma(E2)\approx0.02$ eV or 4.5 single-particle units.

3. Alpha-Particle Width

Our experimental value

$$\Gamma_\alpha=14+3\text{ eV}$$

for the width of the 4.77-MeV level against alpha decay to the ground state of Li^6 can be turned into a reduced alpha-particle width

$$\theta_\alpha{}^2=1.9.$$

In effecting this reduction we have used the radius given by the standard formula $R=1.45(A_1{}^{1/3}+A_2{}^{1/3})$ F. The single-particle units are $\hbar^2/MR^2$. Since low-energy alpha particles of $l=2$ are involved, the penetrability correction is large and rapidly dependent on R. We cannot therefore interpret our result for $\theta_\alpha{}^2$ as meaning other than that the alpha-particle width is large. It may well be consistent with a cluster-like description of the B^{10} state: $Li^6_{\text{g.s.}}$ plus $l=2$ alpha particle. We should not take this too literally because the broad $J^\pi=1^+$ state at about 5.2 MeV appears to be like $Li^6_{\text{g.s.}}$ plus $l=0$ alpha particle[12,13] and the $l=2$ cluster configuration would scarcely be expected below the $l=0$.

It is now interesting to ask whether the IPM has anything to say about $\theta_\alpha{}^2$. The expectation of IPM_{new} is not available on this point but IPM_{old} has been examined in the form developed by Soper to whom we are grateful for the communication of his result. At $a/K=4$ the wave function of the appropriate $J^\pi=3^+$ state contains about 90% by intensity of the partition [442] so we should indeed expect a large alpha-particle width. It would be interesting to have the corresponding figure for IPM_{new}.

4. Comments

The position of the $J^\pi=3^+$ state and its very small ground-state $M1$ width accord very well with the predictions of IPM_{new}. The two strong collective properties, the very large $E2$ width to the first excited state and the alpha-particle width may suggest some form of cluster-rotational behavior based on a Li^6-plus-alpha-particle picture for the 0.72-MeV state. It would be interesting to know the alpha-particle reduced width of the 0.72-MeV state for the ground state of Li^6. There is, of course, no necessary conflict between these two views, IPM and collective, of the states in question but, as already emphasized, it is desirable in that case for the IPM wave functions themselves to favor the $E2$ transition and the large alpha-particle width. As we have seen, the IPM wave functions themselves indeed show a very strong $E2$ transition.

We summarize the questions that our work on the 4.77-MeV level poses for IPM_{new}:

(i) Can the model be reconciled with the tremendous $E2$ width to the 0.72-MeV $J^\pi=1^+$ state?

(ii) Can the model accommodate the very small $E2$ width to the ground state?

(iii) Does the model give a large proportion of the partition [442] in the $J^\pi = 3^+$ state?

If the answer to all those questions is yes, we shall conclude that the model's account of this rather remarkable state is impressively good and that its credibility is thereby strengthened.

B. 5.16-MeV Level of B^{10}

1. Gamma-Ray Widths

We have, combining the present figures for the gamma-ray and the alpha-gamma branching ratio:

$$\Gamma_\gamma = 2.9 \pm 1.1 \text{ eV}.$$

This figure may be combined with the accurate branching ratios earlier determined for this level,[9] assuming, as is reasonable, that there is not a strong undetected transition to the 3.58-MeV level, to give

$$\Gamma_{\gamma(3.01)} = 1.9 \pm 0.7 \text{ eV},$$
$$\Gamma_{\gamma(4.44)} = 0.86 \pm 0.32 \text{ eV},$$
$$\Gamma_{\gamma(5.16)} = 0.16 \pm 0.06 \text{ eV}.$$

We have no immediately unambiguous experimental information on possible $E2$ components. It is likely, however, that the $M1$ components dominate since the single-particle $(1p_{3/2} \rightarrow 1p_{3/2})E2$ strengths for $\langle r^2 \rangle_p = 7.9 \times 10^{-26}$ cm^2 as used previously, are: 1.0×10^{-3}, 7.0×10^{-3}, 1.5×10^{-2} eV for the 3.01-, 4.44-, and 5.16-MeV transitions, respectively. It is therefore improbable that there are significant $E2$ contributions (note that $\Delta T = 1$ so there is no simple collective enhancement).

The angular distribution[6] of these gamma rays in the $Li^6(\alpha,\gamma)B^{10}$ reaction requires $E2/M1$ ratios of 0.01 or 150 by intensity for the 3.01- and 4.44-MeV transitions and 0.02 or 9 for the 5.16-MeV transition. We can confidently reject the larger numbers and so interpret our experimental widths as referring essentially to the $M1$ components. In Table III we compare experiment with IPM_{old} and with both the 17-parameter versions of IPM_{new}, that using $A = 8$ through 16 and that using $A = 6$ through 16. We see that agreement with the model for the 3.01- and 5.16-MeV transitions may be regarded as fairly satisfactory but that for the 4.44-MeV transition is poor. On the other hand we also see from Table III that the 4.44-MeV transition appears to be a very sensitive one, changing in strength by a factor of several hundred as between the two IPM_{new} parametrizations used here. We may therefore perhaps hope that it can be brought into line in the manner discussed in the Introduction. We also see that the account given by IPM_{new} of these absolute transition probabilities is significantly superior to that given by IPM_{old}.

TABLE III. Experimental gamma-ray widths and theoretical $M1$ widths in eV for transitions from the 5.16-MeV state of B^{10}.

Final state (MeV)	Γ_γ(exptl.)	$\Gamma_\gamma(M1)$(theoret.) IPM_{old}	$IPM_{new(8)}$	$IPM_{new(6)}$
2.15	1.9 ±0.7	0.02	0.75	1.1
0.72	0.86±0.32	3.3	0.013	5×10^{-5}
0	0.16±0.06	0.035	0.45	0.083

(In may be significant that in IPM_{old} these transitions are extremely sensitive to a/K where that parameter is small and that some approach to the correct branching ratios and absolute widths can be made, but only at $a/K \approx 2$ which is completely unacceptable from the point of view of the level scheme.)

Since collective enhancements of simple type are absent for these $\Delta T = 1$ transitions the IPM may be expected to give a reasonable account of them. The $E2/M1$ ratios are not yet accurately determined and better measurements are desirable. In the meantime we have rough figures with which we compare the predictions of IPM_{new} in Table IV. Since, according to these figures, the 3.01-MeV transition strength is 20 single-particle units we must view the experimental $E2/M1$ ratios[6] with considerable suspicion and they should be redetermined. However, if the present figures are anywhere near the mark the IPM predictions are very poor. This is at the moment an experimental question.

TABLE IV. Experimental and theoretical $E2$ widths in units of 10^{-3} eV for gamma-ray transitions from the 5.16-MeV state of B^{10}.

Final state (MeV)	$\Gamma_\gamma(E2)$(exptl.)	$\Gamma_\gamma(E2)$(theoret.) $IPM_{new(8)}$	$IPM_{new(6)}$
2.15	20	0.11	0.10
0.72	10	6×10^{-3}	$<3 \times 10^{-3}$
0	3	0.29	0.19

2. Alpha-Particle Width

The $l = 2$ alpha-particle width of the 5.16-MeV state is also obtained by combining the gamma-ray yield datum with that of the alpha-gamma branching ratio:

$$\Gamma_\alpha = 0.44 \pm 0.09 \text{ eV}.$$

Using the same procedures and definitions as discussed above for the 4.77-MeV level this gives:

$$\theta_\alpha^2 \approx 3.5 \times 10^{-4}.$$

This is a very reasonable figure for an isotopic-spin-inhibited transition under the present conditions of excitation and level spacing.[22] It is not possible at this time to compare this figure with any explicit calculation. It would be interesting to compute from the IPM_{new} wave functions the isotopic-spin-mixing Coulomb matrix elements with $J^\pi = 2^+$, $T = 0$ states having large intensities of the partition [442].

3. Comments

The position of this state is well contained in IPM_{new}: $IPM_{new(8)}$ has it at 5.4 MeV and $IPM_{new(6)}$ at 5.2 MeV. As we have just remarked, two of its $M1$ radiative transitions are satisfactorily described by IPM_{new} while the third may well be rather sensitive to the details. The *prima facie* comparison between experiment and theory on the $E2$ widths is very unsatisfactory but the experimental situation is in need of clarification.

We conclude that there is no necessary conflict between IPM_{new} and the experimental properties of this state. We summarize the questions that our work poses for IPM_{new}:

(i) Can the 4.44-MeV transition to the $J^\pi=1^+$ 0.72-MeV state be brought into satisfactory agreement with the scheme?

(ii) What prediction does the model make for the alpha-particle width of the state when the Coulomb perturbation is taken into account?

C. Neighboring States of B^{10}

Three neighboring states to those discussed in this paper require comment. IPM_{new} has given a good account of the positions of the first 7 even-parity states of B^{10} including those at 4.77 and 5.16 MeV. The model has a gap of 1 MeV or so in energy above 6 MeV and it is interesting to ask whether all experimental even-parity states below this gap can be satisfactorily associated with states of the model and, conversely, whether there are any experimental even-parity states in this region of which the model gives no account. (The first single-nucleon threshold in B^{10}, namely Be^9+p, comes at 6.59 MeV and above this the states rapidly become rather broad so that it is difficult to be sure that all have been located experimentally. The presently made examination is therefore probably the limit to which one can exhaustively carry the comparison of theory and experiment.)

IPM_{new} in fact calls for another $J^\pi=2^+$, $T=0$ state below 6 MeV at 5.1 MeV in $IPM_{new(8)}$ and at 5.7 MeV in $IPM_{new(6)}$. In seeking candidates to associate with this model state we must consider first of all that at 5.11 MeV. This state is traditionally held to be of odd parity, the first in B^{10}, and so not to be of interest for the $(1p)^6$ classification. That the traditional view is most probably correct is shown by the reaction $Be^9(d,n)B^{10}$ at $E_d=1.9$ MeV which shows a good plane-wave $l_p=0$ pattern to this state.[23] Although no DWBA fit has been made to the data and the plane-wave pattern for $l_p=1$ also peaks at or near 0° the Q value is low (−0.75 MeV) and under these circumstances experimental distributions usually resemble rather closely the plane-wave patterns in form. This is particularly true when the cross section is large as in this case. The unlikeliness that the 5.11-MeV state can be of $J^\pi=2^+$ is illustrated by the neutron angular distribution leading, under the same experimental conditions, to its $J^\pi=2^+$, $T=1$ neighbor at 5.16 MeV. This angular distribution resembles closely the plane-wave $l_p=1$ pattern and is very different from that for the 5.11-MeV state. We therefore reject the 5.11-MeV state as a candidate for $J^\pi=2^+$.

A $J^\pi=2^+$ state is indeed established experimentally[13] at 5.92 MeV, adequately close to the predicted energy. No absolute gamma-ray yield from the $Li^6(\alpha,\gamma)B^{10}$ reaction is available for this state but it is known[6] to decay predominantly to the ground state. The predictions of $IPM_{new(8)}$ and $IPM_{new(6)}$ as to the relative strength of the ground-state transition are 82 and 99%, respectively. The prediction of IPM_{old} for this proportion is 73%. A measurement of the absolute radiative width of this state and a better figure for the branching to higher states are obviously desirable. It would also be interesting to know the predictions of IPM_{new} about the alpha-particle width of this state. The experimental value[13] is about 0.07 of a single-particle unit. IPM_{old} also predicts a $J^\pi=2^+$ state close to the $J^\pi=3^+$ state but there (in Soper's version) the state contains about 80% of the partition [442] and so should show a larger rather than a modest alpha-particle width. It would be interesting if IPM_{new} as well as accommodating, as it obviously can, the dominating feature of the ground-state radiative transition, also could contain the relatively small alpha-particle width. In the meantime we may tentatively conclude that the 5.92-MeV state is most probably the second $J^\pi=2^+$, $T=0$ state of the IPM and add it provisionally to the list of the successes of IPM_{new}. The $E2/M1$ mixing ratio in the ground-state transition is either 0.01 or 10 by intensity. If the latter, and if the prediction of IPM_{new} as to the $M1$ width were correct, the $E2$ component would have a strength of 25 single-particle units. It would obviously be very interesting to resolve the ambiguity in the mixing ratio in addition to determining the absolute radiative width. IPM_{new} predicts a rather modest $E2$ ground-state transition: for $IPM_{new(8)}$ 0.043 single-particle units unenhanced and 0.17 units enhanced; $IPM_{new(6)}$ is about 10% lower. The model therefore favors the lower value of the $E2/M1$ mixing ratio.

The next state to be considered is the $J^\pi=4^+$, $T=0$ state contained in $IPM_{new(8)}$ at 5.8 MeV and in $IPM_{new(6)}$ at 6.0 MeV. An experimental state with this assignment[6] is found at 6.04 MeV. Again, the absolute gamma-ray yield is not known and again the ground-state radiative transition is dominant. There seems to be no reason for not associating this with the model state although a confrontation of the experimental and theoretical radiative widths is evidently desirable. An

[22] D. H. Wilkinson, in *Proceedings of the Rehovoth Conference on Nuclear Structure*, edited by H. J. Lipkin (North-Holland Publishing Company, Amsterdam, 1958), p. 175.

[23] P. J. Riley, D. W. Braben, and G. C. Neilson, Nucl. Phys. 47, 150 (1963).

interesting experimental fact is that the ground-state transition is predominantly $E2$. If the $M1$ strength is correctly given by $\mathrm{IPM}_{\mathrm{new}}$, the implied $E2$ strength is approximately 3 single-particle units (defined as in the above discussion on the 4.77-MeV state), a very powerful transition. This is to be compared with the strong ground-state transition from the $J^\pi=2^+$ state at 5.92 MeV which may be predominantly $M1$ but may alternatively be predominantly $E2$. In fact $\mathrm{IPM}_{\mathrm{new}}$ correctly predicts a very strong $E2$ ground-state transition from the $J^\pi=4^+$ state: for $\mathrm{IPM}_{\mathrm{new}(8)}$ 1.0 single-particle units unenhanced and 4.2 units enhanced with almost-identical figures for $\mathrm{IPM}_{\mathrm{new}(6)}$.

An indirect approach to the $E2$ components of the ground-state transitions from the 5.92- and 6.04-MeV states comes from the (p,p') reaction at high energy. Such inelastic scattering, in its direct component, follows the $E2$ matrix elements rather closely. It is empirically observed[24] that at a proton energy of 17 MeV the cross section can be used to infer the relative strengths of $E2$ components of radiative widths with a confidence of perhaps a factor of 2 when the transitions are strong. The 6.04-MeV state is indeed excited strongly. In the same (p,p') experiments[24] the 5.92-MeV state is excited weakly relative to the 6.04-MeV state. If the prediction of $\mathrm{IPM}_{\mathrm{new}}$ as to the $M1$ component of the ground-state transition were correct, and if the larger of the two possible $E2/M1$ ratios were correct for the 5.92-MeV state, that state should be excited many times more strongly in the (p,p') reaction than the 6.04-MeV state. This must incline us towards the lower of the alternative $E2/M1$ ratios namely 0.01 in agreement with $\mathrm{IPM}_{\mathrm{new}}$. Similar measurements at a proton energy of 185 MeV[25] excite strongly a state or states in B^{10} at 6.1 ± 0.1 MeV with an angular distribution characteristic of $L=2$. If, as is likely, this refers chiefly to the 6.04-MeV state we can infer the $E2$ strength by comparison with the excitation of the 4.4-MeV C^{12} state seen in the same work with an angular distribution essentially identical with that for the B^{10} state. Using for the radiative width of the C^{12} state the value $(1.1\pm0.2)\times10^{-2}$ eV, the mean of three concordant determinations,[26] gives an $E2$ strength for the B^{10} transition of 3.2 single-particle units in agreement with the prediction of $\mathrm{IPM}_{\mathrm{new}}$ on the $E2$ component and implying agreement with $\mathrm{IPM}_{\mathrm{new}}$ on the $M1$ component.

Further evidence comes from the inelastic scattering to the 6.04-MeV state of electrons of incident energy 100–200 MeV.[27] This shows, in agreement with the results of the $\mathrm{Li}^6(\alpha,\gamma)\mathrm{B}^{10}$ reaction,[6] that the transition is predominantly $E2$ and gives for the radiative width the value, somewhat dependent on details of the charge distribution, $\Gamma_\gamma=0.12\pm0.025$ eV or 3.7 single-particle units. This is in excellent accord with the value derived above from the high-energy (p,p') reaction and confirms the success of $\mathrm{IPM}_{\mathrm{new}}$ for the $E2$ component. This re-emphasizes the need for a model-free determination of the radiative width and a re-determination of the $E2/M1$ mixing ratio to test the apparent success of $\mathrm{IPM}_{\mathrm{new}}$ on the strength of the $M1$ component that appears from the presently available value of that ratio.

This comparison exhausts the states of $\mathrm{IPM}_{\mathrm{new}}$ below the gap at 6 MeV and leaves only one experimental state of even parity unaccounted for by the model, namely, the very broad $J^\pi=1^+$, $T=0$ state at 5.18 MeV.[12] This state may be one of two-particle excitation from the $1p$ shell into the $2s_{1/2}$ shell[28] in which case it is not a candidate for present consideration. However, the radiative width requires consideration. If we combine our present measurements of the absolute gamma-ray yield from the 5.16-MeV level in the same reaction with the relative yields from the 5.16- and 5.18-MeV states[12] we find a radiative width of 0.07 eV for the 3.42-MeV $M1$ transition to the $J^\pi=0^+$, $T=1$ state at 1.74 MeV that, as expected, dominates the radiative decay of the 5.18-MeV level. This is a strength of 0.08 Weisskopf units, a quite usual figure for an isotopic-spin-favored transition and one that may superficially seem to argue against what would nominally be a two-particle jump if the 5.18-MeV level were one of two-particle excitation. $\mathrm{IPM}_{\mathrm{new}}$ contains another $J^\pi=1^+$, $T=0$ state in the region of 7–8-MeV excitation. It would be interesting to know the prediction of the model for the $M1$ radiation of this state to the 1.74-MeV state; the experimental state is very broad and it could have suffered a considerable shift on that account from its unmodified IPM energy. It would also be interesting to know the prediction of the model about the alpha-particle width since the experimental state's width is greater than a single-particle unit.[13]

We need feel no compulsion to fit this state into $(1p)^6$. States of two-particle excitation must come in sooner or later. Indeed the $J^\pi=0^+$, $T=1$ state at 7.56 MeV in B^{10} (6.18 MeV in Be^{10}) has no place in $(1p)^6$ and is most probably such a state. It is then naturally associated with a similar two-particle state of $J^\pi=1^+$, $T=0$ to be expected near 5.18 MeV.[28] The observed $M1$ strength of the $5.18\rightarrow1.74$ MeV transition need not be an impediment to this interpretation since the strength calculated[28] for the $J^\pi=0^+$ to $J^\pi=1^+$ transition, if the two-particle excitation is into the $2s$ shell, is 8.4 Weisskopf units. In this case, an admixture of only 3% by intensity of the two-particle $J^\pi=0^+$ state into the 1.74-MeV state would suffice to account for the observed

[24] G. Schrank, E. K. Warburton, and W. W. Daehnick, Phys. Rev. **127**, 2159 (1962).
[25] D. Hasselgren, P. U. Renberg, O. Sundberg, and G. Tibell, Nucl. Phys. **69**, 81 (1965).
[26] R. H. Helm, Phys. Rev. **104**, 1466 (1956); V. K. Rasmussen, F. R. Metzger, and C. P. Swann, *ibid.* **110**, 154 (1958); H. L. Crannell and T. A. Griffy, *ibid.* **136**, 1580 (1964).
[27] G. Fricke, G. R. Bishop, and D. B. Isabelle, Nucl. Phys. **67**, 187 (1965).
[28] W. W. True and E. K. Warburton, Nucl. Phys. **22**, 426 (1961).

decay. Such an admixture does not seem to be unreasonable. It remains incumbent on the two-particle model to account for the large alpha-particle width of the 5.18-MeV state. On the other hand, no other $J^\pi=1^+$, $T=0$ state to associate with the IPM_{new} state of this assignment has yet been experimentally identified. This remains an open question.

D. Summary of Discussion

With the possible, but not necessary, exception of the $J^\pi=1^+$, $T=0$ state at 5.18 MeV we conclude that the first 10 known even-parity levels of B^{10} are quite well-described by IPM_{new} in respect of their excitations. Conversely, no IPM state in the same region of excitation lacks its experimental identification.

For the 4.77- and 5.16-MeV states, on which we have presented detailed dynamical measurements in this paper, there is no point of necessarily major disagreement with IPM_{new} concerning the $M1$ widths, and there are some striking successes, notably the correct prediction of the very weak ground-state transition from the 4.77-MeV state. Several matters remain to be resolved.

Concerning the $E2$ widths IPM_{new} correctly predicts a very large width for the remarkable transition between the 4.77- and 0.72-MeV levels although it falls short of the experimental value. The model fails badly on the ground-state $E2$ width from this level. For the 5.16-MeV level the experimental situation is unsatisfactory in relation to the $E2$ widths but there are signs that the model may be deficient.

It may be useful to gather together the theoretical and experimental questions of interest that have emerged from our discussion of the 4.77- and 5.16-MeV states and their neighbors.

Theoretical questions for IPM_{new}:

$J^\pi=3^+$, $T=0$, 4.77-MeV state:

1. Can the model accommodate the abnormally strong $E2$ transition to the first excited state?
2. Can the model accommodate the weak $E2$ transition to the ground state?
3. Alpha-particle width?

$J^\pi=2^+$, $T=1$, 5.16-MeV state:

1. Can the strength of the $M1$ transition to the first excited state be adequately increased?
2. Alpha-particle width?

$J^\pi=2^+$, $T=0$, 5.92-MeV state:

1. Alpha-particle width?

Third $J^\pi=1^+$, $T=0$ state:

1. $M1$ width to the 1.74-MeV state?
2. Alpha-particle width?

Experimental questions:

$J^\pi=2^+$, $T=1$, 5.16-MeV state:

1. $E2/M1$ ratios?

$J^\pi=2^+$, $T=0$, 5.92-MeV state:

1. Radiative width?
2. Branching to higher states?
3. $E2/M1$ ratio in the ground-state transition?

$J^\pi=4^+$, $T=0$, 6.04-MeV state:

1. Radiative width?
2. $E2/M1$ ratio in the ground-state transition?

ACKNOWLEDGMENTS AND LOCATIONS OF RESEARCH

Two of us (D.E.A. and R.E.P.) are indebted to Professor S. Gorodetzky for the opportunity of carrying out a portion of this work in collaboration with Dr. A. Gallmann during the summer of 1963. The first-named author wishes to thank the Lockheed Missiles and Space Company for a consulting appointment during which another part of the work was undertaken in collaboration with Dr. L. F. Chase, Jr., and Dr. R. E. McDonald.

We are grateful to Dr. D. Kurath for sending us unpublished data on the $E2$ rates in the independent-particle model.

The coincidence experiments described in Secs. IIA1 and IIA2a were begun at Strasbourg and completed at Brookhaven. Work described in Sec. IIA2b was carried out at Brookhaven. Measurements of alpha-particle singles spectra with a Buechner-type magnetic spectrograph, described in Secs. IIA3 and IIA4 were made at Strasbourg. Experiments on the $Li^6(\alpha,\gamma)B^{10}$ reaction covered in Secs. IIB1, IIB2, IIB5, and IIB6 were done at Brookhaven and the remaining work on this reaction described in Secs. IIB3 and IIB4 was performed at the Lockheed Missiles and Space Company. Self-supporting B^{11} targets were prepared in electron-beam evaporators both at Strasbourg and at Brookhaven. We are indebted to Dr. D. J. Pullen of Oxford University for preparation of the B^{11} targets used in the Buechner spectrograph measurements.